REPORT NO. 132
May, 1960

THE COLLEGE OF AERONAUTICS

CRANFIELD

An Extension of Multhopp's Lifting Surface Theory to Include the Effect of Flaps, Ailerons, etc.

- by -

Robert W. Simpson*, B.A.Sc.

SUMMARY

The subsonic lifting surface theory due to H. Multhopp (Ref. 1) has been extended to include a chordwise discontinuity in the slope of the lifting surface, i.e. to include the effect of flaps, or ailerons. By representing the chordwise loading of a two-dimensional flapped flat plate in closed form, a new loading function ℓ_2 is used in the representation of the chordwise loading, and a new influence function k is defined. This function is dependent on the parameter ϕ_h which describes the hinge position, and so the tabulation which has been done for the influence functions, i and j, in Multhopp's original method have to be repeated for values of ϕ_h.

The method is restricted to linearized, non-viscous flow about thin wings of moderate aspect ratio of any planform. Values of lift, pitching moment and centre of pressure can be obtained across the span for deflected flaps, and the theoretical effect of planform can be studied.

An example has been calculated for a straight rectangular wing of aspect ratio 6 with a full span 20% chord, trailing edge flap. A comparison with available experimental results shows that viscous effects are important in obtaining the correct magnitudes of lift and pitching moments.

---

* Based on a thesis submitted in partial fulfilment of the requirements for the Diploma of the College of Aeronautics.

CONTENTS

LIST OF SYMBOLS

x, y, z — rectangular cartesian co-ordinate system (see Fig. 1)

x_o, y_o — position of inducing station on wing

$\xi = \frac{x}{b/2}$, $\eta = \frac{y}{b/2}$ — non-dimensional co-ordinates related to semispan

$X = \frac{x_o - x_{oL.E.}}{c(y_o)}$, $Y = \frac{Y - Y_o}{c}$ — Non-dimensional wing co-ordinates related to inducing wing section (suffix o)

$X_{oL.E.}$ = position of leading edge of inducing wing section

$\phi = \cos^{-1}(1 - 2X)$ = angular chordwise co-ordinate

$\theta = \cos^{-1}\eta$ = angular spanwise co-ordinate

Note: θ is also used in two-dimensional derivation of flapped plate vorticity distribution as an auxiliary co-ordinate

$\theta = \cos^{-1}\xi$. See Section 3.2

U — velocity of undisturbed flow relative to the wing co-ordinate system

$u, v w$ — perturbation velocities in x, yz directions

α — $-\frac{dz}{dx}(x)$ local wing incidence

α'' — incidence at forward pivotal point, α' -rear pivotal point

P — pressure

ρ — density

ℓ — $\frac{\text{P upper surface - P lower surface}}{\frac{1}{2}\rho U^2}$ = non-dimensional wing loading

b — wing span

c — wing chord

m — number of wing sections taken into account

List of Symbols (Continued)

ν ,n — suffices denoting spanwise stations

ν = pivotal station
n = inducing station

$\theta_\nu = \frac{\pi}{2} - \frac{\nu\pi}{m+1}$ = angular co-ordinate of pivotal stations

$n_\nu = \cos \theta_\nu = \sin \frac{\nu\pi}{m+1}$

$a_{\nu n}$, $b_{\nu n}$ — coefficients for approximate integration

$\gamma = \frac{C_L \cdot c}{2b}$ = non-dimensional lift per unit span

$\mu = \frac{C_M \cdot c}{2b}$ = non-dimensional moment per unit span

i,j,k — influence functions for chordwise downwash integrals

E — % chord for flap

x_h, ϕ_h — position of wing line of flap

δ — angular flap deflection

1. Introduction

The lifting surface theory developed by H. Multhopp[1] produces accurate spanwise distributions of lift C_L and pitching moment C_M for a minimum of computing effort. The method consists of a computing scheme to replace the double integral equation of the lifting surface, using influence functions and carefully selected pivotal points to do the chordwise integration, and an approximate spanwise integration technique similar to Multhopp's treatment of the lifting line problem. The influence functions are tabulated as functions of two variables, X and Y, for any wing, and similar standard coefficients are given for the spanwise integration. The solution of the integral equation is thus reduced to an iterative solution of a set of linear equations.

Multhopp's original paper, summarised briefly at the beginning of the present paper, dealt with steady linearised potential flow about an infinitely thin wing of moderate or large aspect ratio. Garner[3] has extended it to slow pitching oscillations, but oscillatory derivatives, etc. for flutter or high speed oscillations cannot be estimated. The method suggested by Multhopp for dealing with discontinuities in the surface (due to ailerons, flaps, etc.) in Appendix 2 of Ref. 1 is a calculation of equivalent incidences[15] for chordwise discontinuities, and a fairing or interpolation process for spanwise discontinuities.

The present paper deals with wings having discontinuities in the chordwise direction by developing a closed form representation of a flapped plate, and using this as one of the chordwise functional representations. This representation requires the calculation of a new influence function which turns out to be implicitly tied up with the spanwise position of the discontinuity and it is necessary to calculate and tabulate the function for every position of this discontinuity, unless interpolation should prove practical. An example of the calculation of the required coefficients for a 20% flap is included in this report to illustrate the mathematical treatment and to demonstrate that it provides a satisfactory method for the evaluation of the properties of flaps.

2. Theoretical Background

The basic theory of Multhopp[1] is given here to introduce the problem and his nomenclature has been closely followed.

Consider a thin wing in inviscid potential flow. Let (x,y,z) be an orthogonal system of axes such that the x-axis coincides with the direction of the undisturbed flow, and the z-axis is almost perpendicular upwards from the wing area. (Fig. 1).

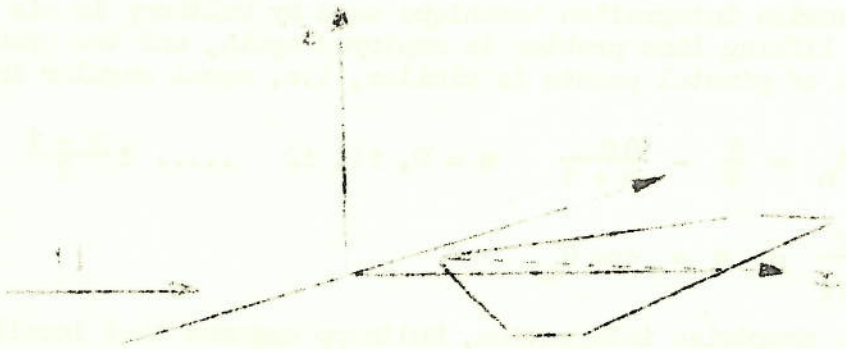

Fig. 1

The perturbations (u,v,w) in velocity due to the wing are assumed small as a necessary condition for the linearisation of the whole problem.

Using the linearised Euler's equations and the continuity equation, and replacing the wing by a discontinuity sheet built from doublets, the relation between local downwash and local loading density for the lifting surface is expressed as :

$$\frac{w(X,Y,Z)}{U} = \frac{-1}{8\pi} \iint_S \frac{\ell(x_o Y_o)}{(y - y_o)^2} \left\{ 1 + \frac{x - x_o}{\sqrt{(x - x_o)^2 + (Y - Y_o)^2}} \right\} dx_o \, dy_o$$

$$\ell(x_o, y_o) = \frac{\Delta P}{\frac{1}{2} \rho U^2} \qquad (1)$$

where x_o, y_o, are positions of doublets and x,y, are general points on the wing.

The double integral equation for $\ell(x_o Y_o)$ has a strong singularity at $y = y_o$; however, a "principal value" can be defined[5].

To satisfy the Kutta-Joukowski condition for smooth flow from the trailing edge, $\ell(x_o y_o)$ is restricted to functions which vanish at the trailing edge.

Since this equation cannot be solved directly, Multhopp constructs linear combinations of independent loading distributions which can be made to satisfy the integral equation at a certain number of "pivotal" points. The more points are taken on the wing, the more independent load distributions can be used, resulting in more accurate results, but the computing effort is proportionally greater.

The spanwise integration technique used by Multhopp in his treatment of the lifting line problem is employed again, and the spanwise distribution of pivotal points is similar, i.e. equal angular increments

$$\theta_n = \frac{\pi}{2} - \frac{n\pi}{m+1} \qquad n = 0, \pm 1, \pm 2 \quad \ldots\ldots \pm \frac{m-1}{2}$$

$$\frac{Y}{b/2} = \eta = \cos\theta_n$$

For the chordwise integration, Multhopp assumes that locally, two-dimensional relationships still hold. He constructs his loading functions $\ell(\phi)$ from terms of the Fourier expansion for thin airfoil theory,

$$\ell(\phi) = a_o \cot\frac{\phi}{2} + \sum_1^\infty a_n \sin n\phi \qquad (2)$$

$$\phi = \begin{cases} 0 & \text{at L.E.} \\ \pi & \text{at T.E.} \end{cases}$$

and chooses his two pivotal stations on the basis of matching expansions of C_L and C_M in terms of α'', α', the incidences at the pivotal points to the thin airfoil results :

$$C_L = \frac{\pi}{2}\left(a_o + \frac{a_1}{2}\right) \qquad (3)$$

$$C_M = -\frac{\pi}{16}(a_1 - a_2) \qquad (4)$$

Thus, C_L and C_M values are estimated as accurately as would be possible with an arbitrary choice of three stations, and the inclusion of another term of the series.

The linear combination for

$$\ell(x_o, y_o) = a_o(y_o)\ell'_o + a_1(y_o)\ell'_1 \qquad (5)$$

is taken by Multhopp as

$$\ell(x_o, y_o) = \frac{2\,C_L}{\pi}(Y_o)\,\ell'_o(x_o) + \frac{8\,C_M}{\pi}(y_o)\,\ell'_1(x_o)$$

$$\text{where } \ell'_o = \cot\frac{\phi}{2}, \quad \ell'_1 = \cot\frac{\phi}{2} - 2\sin\phi$$

$a_o(y_o)$ and $a_1(y_o)$ are weighting functions whose variation with y_o is to be determined. Here they turn out to be expressible as the quantities C_L and C_M using equations (3), (4), (5), accurately represented because of the choice of pivotal points, and whose variation is of practical interest. This is the result of constructing (according to thin airfoil theory) a combination of a "non-lifting moment" distribution $\left[\cot\frac{\phi}{2}\right]$ and a "non-lifting" camber distribution $\left[\cot\frac{\phi}{2} - 2\sin\phi\right]$ which gives the moment.

The integration in the chordwise direction can now be taken to form the influence functions.

$$\frac{w(XYZ)}{U} = -\frac{1}{8\pi}\int_{-b/2}^{b/2}\frac{C_L(Y_o).\,c}{(y-y_o)^2}\left[\frac{2\ell_o(x_o)}{\pi}\left\{1+\frac{x-x_o}{\sqrt{(x-x_o)^2+(y-y_o)^2}}\right\}dx_o\right]dy_o$$

$$-\frac{1}{8\pi}\int_{-b/2}^{b/2}\frac{C_M(Y_o).\,c}{(y-y_o)^2}\left[\frac{8}{\pi}\int_o^c \ell_1(x_o)\left\{1+\frac{x-x_o}{\sqrt{(x-x_o)^2+(y-y_o)^2}}\right\}dx_o\right]dy_o \quad \ldots\ldots (6)$$

where Multhopp defines

$$i(X,Y) = \frac{1}{\pi}\int_o^{\pi}\cot\frac{\phi}{2}\left[1+\frac{X-\frac{1-\cos\phi}{2}}{\sqrt{\left(X-\frac{1-\cos\phi}{2}\right)^2+Y^2}}\right]\sin\phi\,d\phi \quad (7)$$

$$j(X,Y) = \frac{4}{\pi}\int_o^{\pi}\left(\cot\frac{\phi}{2}-2\sin\phi\right)\left[1+\frac{X-\frac{1-\cos\phi}{2}}{\sqrt{\left(X-\frac{1-\cos\phi}{2}\right)^2+Y^2}}\right]\sin\phi\,d\phi$$

$\ldots\ldots$ (8)

and the generalised variables X,Y as :

$$X = \frac{x - x_{L.E.}}{c(y_o)} \qquad Y = \frac{Y - Y_o}{c(y_o)}$$

$$\phi = \cos^{-1}(1 - 2X_o)$$

Combining equation (6) with (7) and (8)

$$\alpha(X,y) = -\frac{1}{2\pi}\int_{-b/2}^{b/2} \frac{C_L\, c(Y_o)\, i(XY) + C_M\, c(Y_o)\, j(XY)}{(y - y_o)^2}\, dy_o \qquad (9)$$

or in non-dimensional variables as defined in the nomenclature

$$\alpha(\xi,\eta) = -\frac{1}{2\pi}\int_{-1}^{1} \frac{\gamma.i + \mu.j}{(n - n^1)^2}\, .\, dn^1 \qquad (10)$$

$$\eta = \frac{Y}{b/2} \qquad n^1 = \frac{Y_o}{b/2}$$

$$\gamma = \frac{C_L c}{2b} \qquad \mu = \frac{C_M c}{2b}$$

The spanwise integration is done by the technique used in Multhopp's treatment[1] of the lifting line problem as described in Section 4 of this report.

The unknown functions $\gamma(n)$, $\mu(n)$ are represented by polynomials in terms of their values at the pivotal points in the usual manner

$$\alpha_\nu(x) = b_{\nu\nu}\,(\gamma i + \mu j)_\nu - \sum_{-(\frac{m-1}{2})}^{\frac{m-1}{2}} b_{\nu n}\,(\gamma i + \mu j)_n \qquad (11)$$

$\nu = n$ not included

where

$$b_{\nu\nu} = \frac{m+1}{4\cos\frac{\nu\pi}{m+1}}\,, \qquad b_{\nu n} = 0 \quad \text{for } |\nu - u| = 2,4,6 \qquad (12)$$

$$b_{\nu n} = \frac{\cos\frac{n\pi}{m+1}}{m+1\,(\sin\frac{n\pi}{m+1} - \sin\frac{\nu\pi}{m+1})} \quad \text{for } |\nu - u| = 1,3,5 \qquad (13)$$

The speed of convergence is dependent on the number of spanwise stations selected; when account is taken of a logarithmic singularity in the integral, the rate of convergence is increased.

Multhopp's method was improved by Mangler and Spencer[2]. This took the form of an addition to the $i_{\nu\nu}$, $j_{\nu\nu}$ terms, and corrected values are denoted $\bar{i}_{\nu\nu}$. $\bar{j}_{\nu\nu}$. The corrected boundary conditions are then expressed as

$$\alpha_\nu(x) = b_{\nu\nu}(\bar{i}_{\nu\nu}\,\gamma_\nu + \bar{j}_{\nu\nu}\,\mu_\nu) - \sum_{-(\frac{m-1}{2})}^{\frac{m-1}{2}} b_{\nu n}\,(i_{\nu n}\,\gamma_n + j_{\nu n}\,\mu_n) \qquad (14)$$

This is satisfied at two points at each pivotal station, denoted by

$$\begin{aligned} x'_\nu &= x_\nu \text{ L.E.} + 0.9045\, c_\nu \\ x''_\nu &= x_\nu \text{ L.E.} + 0.3455\, c_\nu \end{aligned} \qquad (15)$$

From the two conditions at each pivotal station, the unknowns γ_ν , μ_ν are separated by elimination. Thus, the 2m equations are expressed in a more convenient form for solution as follows :-

$$\gamma_\nu = a_{\nu\nu}(\ell'_\nu\,\alpha'_\nu - \ell''_\nu\,\alpha''_\nu) + \sum_{-\frac{m-1}{2}}^{\frac{m-1}{2}} a_{\nu n}\left[(\ell'_\nu i'_{\nu n} - \ell''_{\nu n}\,i''_{\nu n})\gamma_n + (\ell'_\nu j'_{\nu n} - \ell''_\nu j''_{\nu n})\mu_n\right]$$

$$\mu_\nu = a_{\nu\nu}(m''_\nu\,\alpha''_\nu - m'_\nu\,\alpha'_\nu) + \sum_{-(\frac{m-1}{2})}^{\frac{m-1}{2}} a_{\nu n}\left[(m''_\nu\,i''_{\nu n} - m'_\nu\,i'_{\nu n})\gamma_n + (m''_\nu\,j''_{\nu n} - m'_\nu\,j'_{\nu n})\mu_n\right] \qquad \ldots\ldots (16)$$

where

$$\frac{\ell'_\nu}{\bar{j}''_{\nu\nu}} = \frac{\ell''_\nu}{\bar{j}'_{\nu\nu}} = \frac{m'_\nu}{\bar{i}''_{\nu\nu}} = \frac{m''_\nu}{\bar{i}'_{\nu\nu}} = \frac{1}{\bar{i}'_{\nu\nu}\,\bar{j}''_{\nu\nu} - \bar{i}''_{\nu\nu}\,\bar{j}'_{\nu\nu}}$$

The equations are solved by an iterative process whereby even and odd values of n define two sets of equations. This is possible since $a_{\nu n} = 0$ for $|\nu - n| = 2,4,6 \ldots$ Thus, for ν odd, $i_{\nu n}$ need be calculated only for even n, and vice versa.

The aerodynamic forces and moments, their derivatives, and the calculated position of the centre of pressure are obtained from the values of γ_n, μ_n quite readily as suggested by Multhopp,

$$C_L = \frac{\pi A}{m+1} \sum_{-\left(\frac{m-1}{2}\right)}^{\frac{m-1}{2}} \gamma_n \cos \frac{n\pi}{m+1} \qquad (17)$$

$$C_\ell = \frac{\pi A}{m+1} \sum_{-\left(\frac{m-1}{2}\right)}^{\frac{m-1}{2}} \gamma_n \sin \frac{2n\pi}{m+1} \qquad (18)$$

$$X_{a.c.} = \frac{1}{4} - \frac{\mu_n}{\gamma_n}, \qquad n \neq 0 \qquad (19)$$

$$C_M = \frac{\pi A^2}{m+1} \sum_{-\left(\frac{m-1}{2}\right)}^{\frac{m-1}{2}} \left\{ \mu_n \frac{C_n}{b/2} - \gamma_n \left(\frac{X_{nL.E.}}{b/2} + \frac{C_n}{2b} \right) \right\} \cos \frac{n\pi}{m+1} \qquad \ldots\ldots \qquad (20)$$

about the y axis.

This completes a brief summary of Multhopp's paper (R & M 2884). The chordwise pressure distribution has been composed of two special distributions in arbitrary proportions, and the spanwise distribution calculated. The spanwise distribution may be symmetrical, or antisymmetrical (which gives some simplification to calculations) or quite asymmetrical. The only quality the distribution must have spanwise is smoothness. The interpolation functions cannot be expected to work if there is an irregular behaviour between two interpolation stations. Multhopp recommends that the distance between spanwise stations should be less than 0.4 or 0.5 wing chord.

3. Theory

3.1. General

We choose a functional representation for the chordwise loading distribution in Multhopp's method which represents more closely the section loading with a flap deflected. In linearised subsonic theory, the wing loadings can be considered as independent for a flat plate wing at zero incidence with a control flap deflected. The flap represents a discontinuity chordwise in the slope of the wing, and may take any chordwise position, e.g. a nose flap, or a trailing edge flap. As Multhopp has done, we resort to thin airfoil theory to construct this functional representation.

3.2. Vorticity distribution on a flat flapped plate

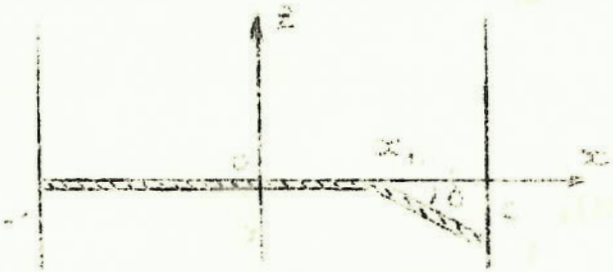

Consider a flat airfoil of chord 2c with z axis as shown in Fig. 2. A trailing edge flap is hinged at X_n and deflected through an angle δ.

Fig. 2

Thin airfoil theory gives the downwash relation

$$w(x,0) = -\frac{1}{2\pi} \oint_{-c}^{c} \frac{\gamma_a(\xi)}{x-\xi} \cdot d\xi \qquad (21)$$

where $\gamma_a(\xi)$ = circulation/unit distance, or vorticity distribution to represent airfoil.

Making the variables dimensionless by putting

$$\bar{x} = \frac{x}{c} \quad , \quad \bar{\xi} = \frac{\xi}{c}$$

we get

$$w(\bar{x},0) = -\frac{1}{2\pi} \oint_{-1}^{1} \frac{\gamma_a(\bar{\xi})}{\bar{x}-\bar{\xi}} \cdot d\bar{\xi} \qquad (22)$$

This equation can be solved for our case by inversion. It is proved by Schugen[17] that for any two functions ψ and g which are continuous except for a finite number of singularities, a unique solution to the integral equation

$$g(x) = \frac{1}{2\pi} \int_{-1}^{1} \frac{\psi(\xi)}{x - \xi} \cdot d\xi \qquad (23)$$

where the variables are dimensionless and $\psi(1)$ is finite or zero, is given by

$$\psi(x) = -\frac{2}{\pi} \sqrt{\frac{1 - x}{1 + x}} \int_{-1}^{1} \sqrt{\frac{1 + \xi}{1 - \xi}} \cdot \frac{g(\xi)}{x - \xi} \cdot d\xi \qquad (24)$$

if $\int_{-1}^{+1} f(\xi)\, d\xi = 0.$

Applying this to equation (21),

$$\gamma_a(\bar{x}) = \frac{2}{\pi} \sqrt{\frac{1 - \bar{x}}{1 + \bar{x}}} \int_{-1}^{1} \sqrt{\frac{1 + \bar{\xi}}{1 - \bar{\xi}}} \cdot \frac{w(\bar{\xi}, 0)}{\bar{x} - \bar{\xi}} \cdot d\bar{\xi} \qquad (25)$$

Now

$$w(\bar{\xi}, 0) = U_\alpha = U \frac{dz(\bar{\xi})}{dx}$$

Therefore,

$$\gamma_a(\bar{x}) = \frac{2U}{\pi} \sqrt{\frac{1 - \bar{x}}{1 + \bar{x}}} \int_{-1}^{1} \sqrt{\frac{1 + \bar{\xi}}{1 - \bar{\xi}}} \cdot \frac{\frac{dz_a}{dx}}{\bar{x} - \bar{\xi}} \cdot d\bar{\xi}$$

In our case (Fig. 2)

$$\frac{dz_a}{dx} = 0 \qquad \text{for } \bar{x} < \bar{x}_h$$

$$= \delta \qquad \text{for } \bar{x} > \bar{x}_h$$

$$\therefore \quad \gamma_a(\bar{x}) = \frac{2U}{\pi}\sqrt{\frac{1-\bar{x}}{1+\bar{x}}}\oint_{\bar{x}_h}^{1}\sqrt{\frac{1+\bar{\xi}}{1-\bar{\xi}}}\cdot\frac{\delta}{\bar{x}-\bar{\xi}}\cdot d\bar{\xi}$$

$$- \frac{2U\delta}{\pi}\sqrt{\frac{1-\bar{x}}{1+\bar{x}}}\oint_{\bar{x}_h}^{-1}\sqrt{\frac{1+\bar{\xi}}{1-\bar{\xi}}}\cdot\frac{d\bar{\xi}}{\bar{x}-\bar{\xi}}$$

If we make the substitution

$$\bar{\xi} = -\cos\theta \qquad \bar{x} = -\cos\phi$$

$$\bar{x}_h = -\cos\phi_h$$

when $\bar{x}$ goes from -1 to 1, ϕ goes from 0 to π

$$d\bar{\xi} = \sin\theta \; d\theta$$

the integral reduces to

$$\int_{\phi_h}^{\pi}\frac{1-\cos\theta}{\cos\theta-\cos\phi}\,d\theta \qquad (26)$$

The value of this integral as obtained in Appendix I is

$$-(\pi-\phi_h) - \frac{(1-\cos\phi)}{\sin\phi}\ln\left|\frac{\sin\frac{\phi_h+\phi}{2}}{\sin\frac{\phi_h-\phi}{2}}\right| \qquad (27)$$

Therefore, $\gamma_a(\bar{x}) = \gamma_a(\phi)$

$$\gamma_a(\phi) = \frac{2U\delta}{\pi}\sqrt{\frac{1+\cos\phi}{1-\cos\phi}}\left[-(\pi-\phi_h) - \left(\frac{1-\cos\phi}{\sin\phi}\right)\ln\left|\frac{\sin\frac{\phi_h+\phi}{2}}{\sin\frac{\phi_h-\phi}{2}}\right|\right]$$

$$= -\frac{2U\delta}{\pi}(\pi-\phi_h)\cot\frac{\phi}{2} - \frac{2U\delta}{\pi}\ln\left|\frac{\sin\frac{\phi_h+\phi}{2}}{\sin\frac{\phi_h-\phi}{2}}\right| \qquad (28)$$

This is the vorticity distribution of a flapped flat plate from 2-D airfoil theory.

3.3. Representation in closed form

To obtain a load distribution we note from linearised theory

$$\frac{P_u - P_L}{\frac{1}{2}\rho U^2} = -\frac{2v}{U} \tag{29}$$

$$\therefore \quad \ell(\phi) = \frac{4\delta(\pi - \phi_h)}{\pi} \cot\frac{\phi}{2} + \frac{4\delta}{\pi} \ln \left| \frac{\sin\frac{\phi_h + \phi}{2}}{\sin\frac{\phi_h - \phi}{2}} \right| \tag{30}$$

This loading function can also be represented [9][10] by a Fourier series of the form

$$\ell(\phi) = a_o \cot\frac{\phi}{2} + \sum_1^\infty a_n \sin n\phi \tag{31}$$

where

$$a_o = \frac{4(\pi - \phi_h)}{\pi}\delta$$

$$a_n = \frac{8 \sin n\phi_h}{\pi}\delta \tag{32}$$

and the usual thin airfoil relations apply :

$$C_L = \frac{\pi}{2}\left(a_o + \frac{a_1}{2}\right)$$

$$C_M = -\frac{\pi}{16}(a_1 - a_2) \tag{33}$$

Thus we see that we have obtained the series summation in closed form. The $\cot\frac{\phi}{2}$ term may be taken as the flat plate distribution due to an induced angle of attack caused by the flap deflection. The logarithmic term represents the distribution due to camber line shape, and has a singularity at the hinge position.

Using relations (33)

$$C_L = 2\delta\,(\pi - \phi_h + \sin\phi_h) \tag{34}$$

and

$$C_M = -\frac{\delta}{2}(1 - \cos\phi_h)\sin\phi_h$$

Now, if E denotes the % chord of a trailing edge flap (Figs. 2 and 3) $(1 - E) = \frac{1 - \cos \phi_h}{2}$

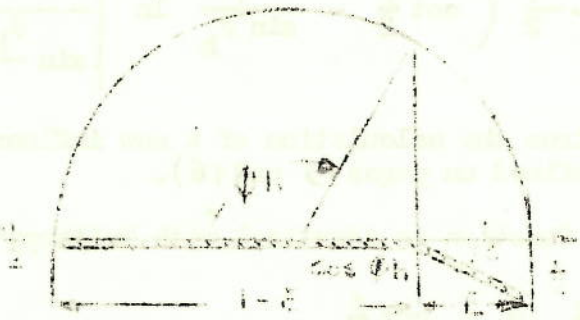

Fig. 3

In terms of a_1,

$$C_M = -\frac{\pi}{8}(1 - E)a_1 \qquad (36)$$

C_H, a_2, b_2, etc., are calculated in Appendix III.

3.4. Construction of the loading functions

Following Multhopp, we construct two chordwise loading distributions: one giving lift and no moment; the other a moment but no lift. This is done in order that the spanwise distribution of C_L and C_M will be a direct result of the solution of the equations.

The functions we choose are the $\cot \frac{\phi}{2}$ term, and the logarithmic function. Since this logarithmic loading has a lifting contribution, we add a negative $\cot \frac{\phi}{2}$ contribution to get a zero lift representation with the same C_M value.

Considering a loading of the general form

$$\ell(\phi) = a_o \cot \frac{\phi}{2} + \sum_1^\infty a_n \sin n\phi$$

then C_L will always be zero if

$$C_L = \frac{\pi}{2}\left(a_o + \frac{a_1}{2}\right) = 0$$

$$\text{i.e. } a_o = -\frac{a_1}{2} = -\frac{4\delta}{\pi} \sin \phi_h \qquad (37)$$

Therefore, the new functional representation chosen is

$$\ell_2(\phi) = -\frac{a_1}{2}\left(\cot\frac{\phi}{2} - \frac{1}{\sin\phi_h}\ln\left|\frac{\sin\frac{\phi_h+\phi}{2}}{\sin\frac{\phi_h-\phi}{2}}\right|\right) \quad (38)$$

This loading requires the calculation of a new influence function denoted by "k" (defined on pages 15 and 16).

The other loading function is identical with Multhopp's,

$$\ell_o = A_o \cot\frac{\phi}{2}$$

$$C_L = \frac{\pi A_o}{2}$$

A_o is quite general. They theory can be applied to flapped wings at incidence. (Incidence being measured as $\frac{\partial z}{\partial \alpha}$). We can use the influence function "i", as tabulated by Multhopp for this loading.

Thus, we have replaced the continuous loading function by a linear combination of the form:

$$\ell(x_o, y_o) = \frac{2\,C_L(Y_o)}{\pi} \cdot \ell'_o(x_o) + \frac{4\,C_M(Y_o)}{\pi(1-E)}\,\ell'_2(x_o) \quad (40)$$

where ℓ'_o, ℓ'_2 are purely functional representations.

3.5. Choice of Pivotal Points

We are taking two independent load distributions, and therefore need two pivotal points at each chordwise station. Multhopp selected the position of these points on the basis of using the first two terms of the Fourier expansion to give accurate estimations of the values of C_L and C_M, and the same positions have been chosen here; namely,

$$x' = x_{L.E.} + 0.9045c\,, \qquad \phi'_1 = \frac{4\pi}{5}$$

$$x'' = x_{L.E.} + 0.3455c\,, \qquad \phi''_1 = \frac{2\pi}{5}$$

where c is the local chord. It should be noted that they are well away from the hinge position (Fig. 4).

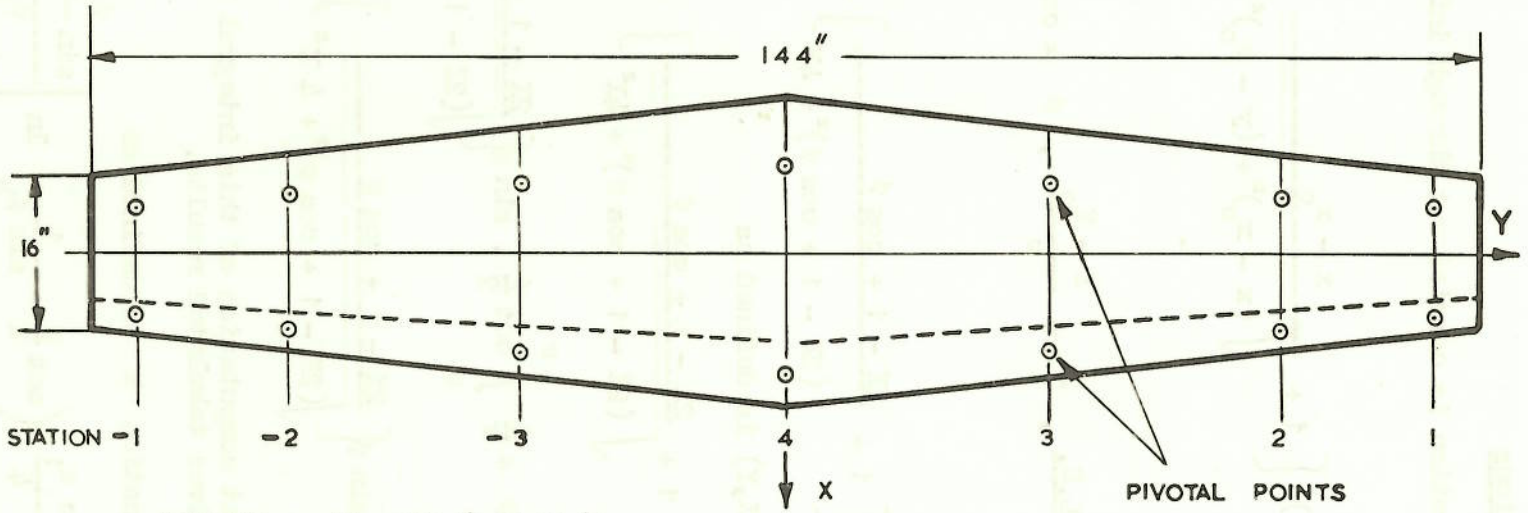

SECTION - 66 - 116 ($a = 0 \cdot 6$)
20% SPLIT FLAP
TAPER 2:1

FIG. 4. WING OF EXAMPLE CALCULATION N A C A T.N. 1759
SCALE : 1" = 20"

3.6. The influence functions

The chordwise integration is carried out through influence functions of the form :

$$\int_{L.E.}^{T.E.} \ell(\phi) \left\{ 1 + \frac{x - x_o}{\sqrt{(x - x_o)^2 + (y - y_o)^2}} \right\} dx_o$$

Using the co-ordinates

$$X = \frac{x - x_{oL.E.}}{c} , \quad Y = \frac{Y - Y_o}{c} , \quad \phi = \cos^{-1}(1 - 2X_o)$$

this becomes

$$\frac{c}{2} \int_o^{\pi} \ell(\phi) \left\{ 1 + \frac{2X - 1 + \cos\phi}{(2X - 1 + \cos\phi)^2 + 4Y^2} \right\} \sin\phi . \, d\phi$$

The influence function $i(X,Y)$ is defined as

$$\frac{1}{C_L c} \int_o^{\pi} \frac{c}{2} . a_o \cot\frac{\phi}{2} \left\{ 1 + \frac{2X - 1 + \cos\phi}{\sqrt{(2X - 1 + \cos\phi)^2 + 4Y^2}} \right\} \sin\phi . \, d\phi$$

$$= \frac{1}{\pi} \int_o^{\pi} \cot\frac{\phi}{2} \sin\phi . \, d\phi + \frac{1}{\pi} \int_o^{\pi} \cot\frac{\phi}{2} . \sin\phi \left\{ \frac{2X - 1 + \cos\phi}{\sqrt{(2X - 1 + \cos\phi)^2 + 4Y^2}} \right\} d\phi$$

$$= 1 + \frac{1}{\pi} \int_o^{\pi} \cot\frac{\phi}{2} . \sin\phi \left\{ \frac{2X - 1 + \cos\phi}{\sqrt{(2X - 1 + \cos\phi)^2 + 4Y^2}} \right\} d\phi \qquad (41)$$

Multhopp suggests that computation of this integral be done by graphical means, and he gives tabulated results.

Our new influence function k is defined as

$$k(X,Y,\phi_h) = \frac{1}{C_M c} \int_o^{\pi} - \frac{c\, a_1}{4} \left(\cot\frac{\phi}{2} - \frac{1}{\sin\phi_h} \ln \left| \frac{\sin\frac{\phi_h + \phi}{2}}{\sin\frac{\phi_h - \phi}{2}} \right| \right)$$

$$\left\{ 1 + \frac{2X - 1 + \cos\phi}{\sqrt{(2X - 1 + \cos\phi)^2 + 4Y^2}} \right\} \sin\phi . \, d\phi$$

$$= \frac{2}{\pi(1-E)} \int_0^{\pi} \left(\cot\frac{\phi}{2} - \frac{1}{\sin\phi_h} \cdot \ln \left| \frac{\sin\frac{\phi_h+\phi}{2}}{\sin\frac{\phi_h-\phi}{2}} \right| \right)$$

$$\left\{ 1 + \frac{2X - 1 + \cos\phi}{\sqrt{(2X-1+\cos\phi)^2 + 4Y^2}} \right\} \sin\phi \, d\phi$$

..... (42)

This is reduced to the form (See Appendix II)

$$k = \frac{2}{1-E} \left[i(X,Y) - 1 - \frac{K}{\pi \sin\phi_h} \right] \qquad (43)$$

where

$$K = \int_0^{\pi} \ln \left| \frac{\sin\frac{\phi_h+\phi}{2}}{\sin\frac{\phi_h-\phi}{2}} \right| \sin\phi \left\{ \frac{2X - 1 + \cos\phi}{\sqrt{(2X-1+\cos\phi)^2 + 4Y^2}} \right\} d\phi$$

..... (44)

The value of K would seem to be best evaluated by graphical means. The logarithmic function has a singularity at the hinge position, but graphical integration is possible (see Figs. 11 - 16).

It is important to notice that ϕ_h adds a new parameter to the calculation of the influence function, and it cannot vary in its chordwise position unless a complete set of k functions are calculated. The value of δ has however been taken outside the calculation of the influence function, and lies explicitly in the values of C_L, C_M at each station. An induced flap angle δ is presumed to exist to allow for the spanwise variation of these quantities.

3.7. The calculation of k

From $$k = \frac{2}{1-E} \left[i(XY) - 1 - \frac{K}{\pi \sin\phi_h} \right]$$

i(X,Y) can be found from tabulated results in Ref. 1; K can be evaluated by graphical integration.

$$K = \int_0^{\pi} \ln \left| \frac{\sin\frac{\phi_h+\phi}{2}}{\sin\frac{\phi_h+\phi}{2}} \right| \left\{ \frac{2X - 1 + \cos\phi}{\sqrt{(2X-1+\cos\phi)^2 + 4Y^2}} \right\} \sin\phi \, d\phi \qquad (45)$$

The bracketted term (or the induction term) is independent of ϕ_h and can be calculated for values of X and Y. The logarithmic term must be calculated for a particular value of ϕ_h (see Table 1). This expression can be simplified for purposes of calculation to the form

$$\ln \left| \frac{A \cos\frac{\phi}{2} + B \sin\frac{\phi}{2}}{A \cos\frac{\phi}{2} - B \sin\frac{\phi}{2}} \right|$$

where

$$A = \sin\frac{\phi_h}{2} \quad \text{and} \quad B = \cos\frac{\phi_h}{2}$$

The product is plotted against ϕ as shown typically in Figs. 5 - 10 to give an idea of the range of values and then integrated by a planimeter. A check of graphical results with exact integration reveals an accuracy of the order of 1%.

The calculation of $k_{\nu\nu}$ requires special treatment. In this case $y = 0$, and the bracketted term becomes either 2 or 0.

$$\left\{ 1 + \frac{2X - 1 + \cos\phi}{\pm (2X - 1 + \cos\phi)} \right\} \quad \begin{matrix} = 2 & X_o < X \\ = 0 & X_o > X \end{matrix}$$

If we associate ϕ_1 with X, i.e. $\cos\phi_1 = 1 - 2X$ then the term has the value 2 for $\phi < \phi_1$

$$\therefore \quad k(X,0) = \frac{2}{\pi(1-E)} \int_0^{\phi_1} \left(\cot\frac{\phi}{2} - \frac{1}{\sin\phi_h} \cdot \ln \left| \frac{\sin\frac{\phi_h + \phi}{2}}{\sin\frac{\phi_h - \phi}{2}} \right| \right) \{ 2 \} \sin\phi \, d\phi$$

and this, using Appendix I reduces to

$$= \frac{4}{\pi(1-E)} \left[\sin\phi_1 - \left(\frac{\cos\phi_h - \cos\phi}{\sin\phi_h} \right) \ln \left| \frac{\sin\frac{\phi_h + \phi}{2}}{\sin\frac{\phi_h - \phi}{2}} \right| \right] \qquad (46)$$

Thus $k_{\nu\nu}$ may be calculated analytically if the positions of the pivotal points ϕ_1, and hinge position ϕ_h are known.

3.8. The spanwise integration

With the definitions of our chordwise loadings, equation (9) becomes

$$\alpha\,(X,Y) = -\frac{1}{8\pi}\int_{-b/2}^{b/2} \frac{C_L\, c(Y_o).\, i(xy.y_o) + C_M\, c(Y_o).\, k(xy\, y_o \phi_h)}{(y - y_o)^2} \,.\, dY_o \qquad \ldots\ldots \quad (47)$$

Introducing non-dimensional terms to proceed with the integration technique,

$$\left.\begin{aligned} \gamma &= \frac{\Gamma}{bu} = \frac{C_L.c}{2b}\,, \qquad \mu = \frac{C_M.c}{2b}\,, \\ \eta &= \frac{Y}{b/2}\,, \qquad \xi = \frac{x}{b/2} \end{aligned}\right\} \qquad (48)$$

Then (47) becomes

$$\alpha(\xi,\eta) = -\frac{1}{2\pi}\int_{-1}^{1} \frac{\gamma(\eta_o).\, i(\xi_1,\eta,\eta_o) + \mu(\eta_o).\, k(\xi_1,\eta,\eta_o,\phi_h)}{(\eta - \eta_o)^2}\, d\eta_o \qquad (49)$$

with the techniques described in Section 5 of Ref. 1, Multhopp reduces the solution of this integral equation to the solution of a set of simultaneous linear equations of the form,

$$\alpha_\nu = b_{\nu\nu}\left[\bar{i}_{\nu\nu}\,\gamma_\nu + \bar{k}_{\nu\nu}\mu_\nu\right] - \sum_{-(\frac{m-1}{2})}^{\frac{m-1}{2}} b_{\nu n}\,(i_{\nu n}\gamma_n + k_{\nu n}\,\mu_n) \qquad (50)$$

where $\bar{i}_{\nu\nu}$ and $\bar{k}_{\nu\nu}$ are values corrected for the logarithmic singularity in the expansion of the influence functions with respect to Y. These equations may be transformed into equations for γ_ν and μ_ν and the solution done by iteration as originally done in Multhopp's paper.

Generally, the number of points will be fifteen or more for good accuracy, so that discontinuities in flap in this direction can be handled more easily. This discontinuity will appear in α', the rearward pivotal station slope, and this value can be faired by the method suggested by Multhopp for interpolation purposes. However, if the discontinuity is inboard, an excessive number of points may be necessary.

The loading spanwise may be symmetrical or antisymmetrical, so that flaps or aileron cases can be calculated:- there is a slight difference in the solutions.

3.9. Correction for the logarithmic singularity

Multhopp has pointed out that in expanding the influence functions for small values of Y, an additional term should be added due to the logarithmic singularity arising from the expansion of the induction term. (See Appendix 13, Ref. 1). He used distributions of vorticity which are regular across the chord, and included an additional term as a correction to the $i_{\nu\nu}$ term. Mangler and Spencer[2] have given a better form of this correction as

$$\Delta i_{\nu\nu} = 4 k_1 \left(\frac{b}{x_\nu}\right)^2 F.(\theta)$$

where $F(\theta)$ is given for a number of spanwise pivotal stations.

In this case, we have a loading distribution which is logarithmic, and has an isolated singularity at the point $\phi = \phi_h$:

$$\ln \left| \frac{\sin \frac{\phi_h + \phi}{2}}{\sin \frac{\phi_h - \phi}{2}} \right| = \sum_1^\infty \frac{2 \sin n \phi_h}{\pi n} \sin n \phi$$

This function can be represented by a Fourier series, and is quite regular except at the point $\phi = \phi_h$. It is reasonable therefore that we may proceed as Multhopp has done, unless one of the pivotal stations happens to coincide with the flap hinge point. The pivotal point is placed on the flap to avoid this circumstance.

Then, we can evaluate the k term

$$k_3 = -\frac{1}{C_M} \cdot \frac{d\, \ell_2 (X)}{d(X_o)} = -\frac{1}{C_M} \cdot \frac{1}{\sin\phi} \cdot \frac{d\, \ell_2 (\phi_1)}{d\, \phi/2}$$

But $C_M = -\frac{\pi}{8}(1 - E)a_1$

$$= \frac{-4}{\pi(1 - E) \sin\phi} \cdot \frac{d}{d\phi/2} \left[\cot \frac{\phi}{2} - \frac{1}{\sin \phi_h} \cdot \ln \left| \frac{\sin \frac{\phi_h + \phi}{2}}{\sin \frac{\phi_h - \phi}{2}} \right| \right]$$

$$= \frac{-4}{\pi(1 - E) \sin\phi} \left[\operatorname{cosec}^2 \frac{\phi}{2} + \frac{1}{\sin\phi_h} \frac{2 \sin\phi_h}{\cos\phi_h - \cos\phi} \right]$$

See Appendix I.4

$$= \frac{4}{\pi(1 - E)\sin\phi} \left[\operatorname{cosec}^2 \frac{\phi}{2} - \frac{2}{\cos\phi_h - \cos\phi} \right] \quad \phi = \phi_1$$

where ϕ_1 describes the pivotal position.

4. Example Calculation

4.1. Method

To ensure that there are no unexpected difficulties in using a logarithmic function for chordwise loading, a simple calculation has been attempted for a single planform for which experimental results are available[6]. The wing selected is rectangular, unswept, with full span, split flaps of 20% wing chord (see Fig. 4).

Two chordwise points, and seven stations across the span have been used. Since the flaps are full span, we can expect no appreciable irregular spanwise distributions due to the small number of stations.

The calculation of k is made for 20% chord, or $\phi_h = 126.9^\circ$. First, the values of X, Y are calculated and tabulated in Tables 3 and 4. For each pivotal point, the value of K is obtained by graphical integration which is illustrated in this report by a typical set of graphs* drawn in Figs. 5 - 10 based on calculations such as Table 2 and tabulated in Table 8. The values of i(X,Y) are given in Table 6 from Ref. 1, and the forms of calculation follow that suggested there.

The values of $k(X', 0)$, and $k(X'', 0)$ may be evaluated (see Table 5).

$$k(X',0) = \frac{4}{\pi(1-E)} \left[\sin\frac{4\pi}{5} - \left(\frac{\cos 126.9^\circ - \cos\frac{4\pi}{5}}{\sin 126.9^\circ} \right) \ln. \left| \frac{\sin 135.4^\circ}{\sin 8.5^\circ} \right| \right]$$

$$= .286$$

Similarly, $k(X'',0) = 2.88$

The values of k_3' , k_3'' can also be calculated for use in the correction to k_{vv} for the logarithmic singularity.

---

* The original thesis contained a complete set of tables and figures for the whole range of values of k, samples only being reproduced here.

$$k_3 = \frac{4}{\pi(1-E)\sin\phi}\left[\operatorname{cosec}^2\frac{\phi}{2} - \frac{2}{\cos\phi_h - \cos\phi}\right]\phi = \phi_1$$

$$k'_3 = \frac{4}{.8\pi\sin\frac{4\pi}{5}}\left[\frac{1}{\sin^2\frac{2\pi}{5}} - \frac{2}{-.6-\cos\frac{4\pi}{5}}\right] = -22.7$$

$$k''_3 = \frac{4}{.8\pi\sin\frac{2\pi}{5}}\left[\frac{1}{\sin^2\frac{\pi}{5}} - \frac{2}{-.6-\cos\frac{2\pi}{5}}\right] = 8.50$$

Thus the values of $\bar{k}_{\nu\nu}$ can be estimated. The so-called correction terms are really additional terms, and the value of $\Delta k_{\nu\nu}$ obtained here is five times the value of $k_{\nu\nu}$. The corrections are made in Table 7.

Form I and II (Tables 10 - 12) deal with the calculation of the values of $B_{\nu n}$, $C_{\nu n}$, $D_{\nu n}$ and $E_{\nu n}$ given in Tables 13 and 14. The problem then reduces to the iterative solution of equations of the form

$$\gamma_\nu = a_{\nu\nu}\left(\ell'_\nu\,\alpha'_\nu - \ell''_\nu\,\alpha''_\nu\right) + \sum_0^{\frac{m-1}{2}} B_{\nu n}\,\gamma_n + \sum_0^{\frac{m-1}{2}} C_{\nu n}\,\mu_n$$

$$\mu_\nu = a_{\nu\nu}\left(m''_\nu\,\alpha''_\nu - m'_\nu\,\alpha'_\nu\right) + \sum_0^{\frac{m-1}{2}} D_{\nu n}\,\gamma_n + \sum_0^{\frac{m-1}{2}} E_{\nu n}\,\mu_n$$

A shortened form of this solution is given for $\alpha' = 2$, $\alpha'' = 1$ in Tables 16 and 17, and summarised and checked in Table 15. For $\alpha' = 1$, $\alpha'' = 0$, the solution is given in Tables 19 and 20 and summarised and checked in Table 18.

The actual solution of these equations is fairly simple in this case compared to the amount of work involved in caclulating the coefficients $B_{\nu n}$, etc. Thus, many calculations can be more readily made once the coefficients are evaluated for a given wing.

4.2. Results

The results of the calculation are shown in Figs. 12 to 16 and Tables 21 - 23.

The spanwise distributions of C_L are shown in Fig. 13 for zero incidence and $\alpha = 6.7^\circ$. This latter result has been obtained by linearly interpolating the difference in the zero and unit incidence calculations. Similarly $\frac{\partial C_L}{\partial \alpha}$ is estimated as 3.89/radian.

The distribution for equal integrated C_N and C_L values is shown in Fig. 14. A similar model comparison is made in Fig. 12 where the centreline ordinate has been taken as unity. Experimental results are compared with a lifting line solution by Multhopp's method, and those calculated by the theory of this paper.

The spanwise distribution of C_M is shown in Fig. 15 and there are no comparable experimental data.

The centres of pressure are plotted in Fig. 16. An experimental check is not possible, and the comparison is made with thin airfoil theory estimations.

4.3. Discussion of results

The results of the calculations do not agree quantitatively with the results of Ref. 6. This would be expected since the effects of viscosity are neglected, and a split flap was used in that investigation. Comparing the zero incidence, flap deflected, results, we see that experimental results are approximately 60% of the theoretical estimations. It is well known that results from two-dimensional thin airfoil theory for flapped controls is generally 20% too high.

Making the comparison at 6.7°, or an experimental C_N of 1.60, there is again a considerable difference, but that it is almost the same as at zero incidence. This suggests that the experimental difference is due mainly to viscous effects on the flap. Thus, it would seem that a better estimation could be made if flap effectiveness could be accounted for by empirical or experimental means. The information input to the equations could be modified by using an effective flap angle $\tau\delta$ instead of δ, so that

$$\alpha' = \alpha'' + \tau\delta$$

The distribution of lift across the span agrees more closely with lifting line theory than the experimental results as seen in Fig. 12. However, it must be remembered that rather few spanwise points have been taken in both calculations, and that the experimental values have not been corrected for wind tunnel interference.

The distribution of moment shows a change of shape for the two incidences, but not much change in overall magnitude. If the lift and moment distributions were independent we would expect that the shape would be the same in both calculations, but it is obvious from the equations

$$\mu_\nu = a_{\nu\nu}\,(m''_\nu\,\alpha''_\nu - m'_\nu\,\alpha'_\nu) + \sum_0^{\frac{m-1}{2}} D_{\nu n}\,\gamma_n + \sum_0^{\frac{m-1}{2}} E_{\nu n}\,\mu_n$$

$$= a_{\nu\nu}\,(m''_\nu - m'_\nu)\,\alpha - a_{\nu\nu}\,m'_\nu\,\delta + \sum_0^{\frac{m-1}{2}} D_{\nu n}\,\gamma_n + \sum_0^{\frac{m-1}{2}} E_{\nu n}\,\mu_n$$

where $\alpha'' = \alpha$, $\alpha' = \alpha + \delta$

that the distribution of moment depends on the incidence $\alpha''$and the lift distribution γ_n . The main contribution to μ_n comes from the $a_{\nu\nu}(m''_\nu \alpha''_\nu - m'_\nu \alpha'_\nu)$ term, and so we see the variation in μ_n is mainly dependent on the value od $m''_\nu - m'_\nu$ which modifies the α value. For a variation of α of one radian, the change of shape is apparent, but the overall magnitude has not changed very much. This variation in C_M with incidence is due to the fact that the aerodynamic centre no longer coincides with the quarter chord point when the flap is deflected.

The theoretical centre of pressure shows fair agreement with two-dimensional values, and some slight variation from a straight line for the zero incidence case.

5. General Discussion of Theory

To satisfy the integral equation at a limited number of pivotal stations would only be justifiable if the boundary conditions, i.e. $\alpha(x,y)$, are fairly continuous. To overcome this, we have chosen an $\alpha(xy)$ distribution which is discontinuous at the hinge point, and constant over each portion of chord, i.e. a flat flapped plate. The functional representation of this has been obtained in closed form so that all terms of the thin airfoil series expansion are included, but only two pivotal stations are required, one on each portion of the wing. Since the points chosen by Multhopp would be used presumably for a wing without flaps, these have been retained to reduce extra calculations. Generally, these points will satisfy this condition for trailing edge flaps since the rearward point lies at 90% chord. Other choices may be necessary for leading edge flaps.

The method describes the flow over wings of low or moderate aspect ratio, and any given planform. The effects of leading edge, trailing edge flaps, or ailerons on low aspect ratio straight wings, swept wings, or delta wings, may be indicated. Part span controls could also be treated if enough spanwise points were taken to describe the irregularities in the spanwise distributions.

In estimating the effects of these controls on actual wings, the effect of viscosity would be rather marked, and limits the usefulness of the calculation. The quantities $\frac{\partial C_M}{\partial C_L}$, $\frac{\partial C_L}{\partial \alpha}$ would be the only valuable result expected from the theory, unless experimental evidence can suggest an empirical modification to the flap angle used. The trend towards laminarised flow wings with simple controls may reduce the magnitude of this error in future. Flap blowing would also reduce the size of this error.

There is a coupling between the distributions obtained from the equations, which suggests that the loadings are not independent. A cambered, flapped wing may therefore require a calculation involving three pivotal points. Further theoretical calculations with available experimental checks should be done to investigate this matter, and to verify the use of an effective flap angle.

6. Conclusions

By representing the flapped flat plate distribution of thin airfoil theory in closed form, Multhopp's method has been extended to account for a discontinuity in surface slope in the chordwise direction. This permits effects of leading edge flaps, trailing edge flaps, and ailerons on wings of any planform to be calculated by what is considered to be a more accurate method than that suggested by Multhopp.

However, for quantitative agreement, empirical or experimental data must be used to allow for the effects of viscosity in the real case. In view of the large amount of necessary calculation, this fact weakens the argument for using such a calculation. The effects of flap or aileron deflection on different planforms will be indicated in a qualitative fashion, and the values of $\frac{\partial C_L}{\partial \alpha}$, $\frac{\partial C_M}{\partial C_L}$ may be quite representative.

The computing effort involved would be reduced if the influence function k were tabulated. Unfortunately, its dependence on the parameter ϕ_h, the position of the wing line of the flap, renders this impractical, unless interpolation is possible, or representative values used. The method outlined in this paper can be useful in the evaluation of the properties of flaps.

7. Acknowledgements

The author acknowledges with gratitude the assistance of Mr. W. Rainbird, who supervised the work, and of Mr. J. L. Naylor who edited the paper for publication.

7. References

1.	Multhopp, H.	Methods for Calculating the Lift Distribution of Wings (Subsonic Lifting Surface Theory). R & M 2884
2.	Mangler, K.W., Spencer, B.F.R.	Some Remarks on Multhopp's Subsonic Lifting Surface Theory. R.A.E. TN. Aero 2181.
3.	Garner, H.C.,	Multhopp's Subsonic Lifting Surface Theory of Wings in Slot Pitching Oscillations. R & M 2885.
4.	Garner, H.C.	Swept Wing Loading: A Critical Comparison of Four Subsonic Vortex Sheet Theories. A.R.C. 14138 C.P.102.
5.	Mangler, K.W.	Improper Integrals in Theoretical Aerodynamics. A R.C. 14394 C.P.94.
6.	West, F.E. Jr., Hallissy, J.M. Jr.	Effects on Compressibility on Normal Force Pressure, and Load Characteristics of a Tapered Wing of NACA 66 - series Airfoil Sections with Split Flaps. NACA TN.1759
7.	Falkner, V.M., Watson, E.J.	Tables of Multhopp and other Functions for use in Lifting Line and Lifting Plane Theory. R & M 2593.
8.	Vandrey, F.	Graphical Solution of Multhopp's Equations for Lift Distribution of Wings. A.R.C. 14238 C.P.96.
9.	Glauert, H.	Theoretical Relationships for an Airfoil with a multiply Hinged Flap System. R & M 1095.
10.	Perring, W.G.A.	The Theoretical Relationships for an Airfoil with a Multiply Hinged Flap System. R & M 1171.

References (Continued)

11.	Brebner, G.G., Lemaire, D.A.	The calculation of the Spanwise Loading of Sweptback Wings. R.A.E. Report Aero 2553.
12.	Bisplinghoff, Ashley, Halfman.	Aeroelasticity. Addison-Wesley Publishing Co. 1955.
13.	Pope, A.	Wing and Airfoil Theory. McGraw Hill. 1951.
14.	Durand, W.F.	Aerodynamic Theory. Vol. II.
15.	Falkner, V.M.	The Use of Equivalent Slopes in Vortex Lattice Theory. R & M 2293
16.	Curtis, A.R.	Tables of Multhopp's Influence Functions. NPL Math. Div. Report Ma/21/(5)5 May,1952.
17.	Söhngen, H.	Die Losungen der Integral gleichung und deren Anwedung in der Traflugel theorie. Math. Bond 45 - 1939.

APPENDIX I

(1) The Evaluation of the Integral

$$\int_{\phi_h}^{\pi} \frac{1 - \cos\theta}{\cos\theta - \cos\phi} \cdot d\theta$$

$$= \int_{\phi_h}^{\pi} \frac{d\theta}{\cos\theta - \cos\phi} - \int_{\phi_h}^{\pi} d\theta - \int_{\phi_h}^{\pi} \frac{\cos\phi \cdot d\theta}{\cos\theta - \cos\phi}$$

$$= -(\pi - \phi h) + (1 - \cos\phi) \int_{\phi_h}^{\pi} \frac{d\theta}{\cos\theta - \cos\phi}$$

The integral $\int_{\phi_h}^{\pi} \frac{d\theta}{\cos\theta - \cos\phi}$ is similar to Glauert's integral, and is evaluated in the following manner.

Noting that $\frac{1}{\cos\theta - \cos\phi}$ can be put in the form

$$\frac{1}{2\sin\phi} \left[\cot\frac{(\theta + \phi)}{2} - \cot\frac{(\theta - \phi)}{2} \right]$$

and that

$$d\left(\frac{\theta + \phi}{2}\right) = d\left(\frac{\theta - \phi}{2}\right) = \frac{d\theta}{2}$$

$$\therefore \int \frac{d\theta}{\cos\theta - \cos\phi} = \frac{1}{\sin\phi} \ln \left| \frac{\sin\frac{\theta + \phi}{2}}{\sin\frac{\theta - \phi}{2}} \right| + C$$

Since the denominator passes through zero when $\theta = \phi_1$, we integrate from θ_h to $\phi - \epsilon$, and $\phi + \epsilon$ to π, and take the limit as $\epsilon \to 0$.

Now $$\int_{\phi_h}^{\phi-\epsilon} \frac{d\theta}{\cos\theta - \cos\phi} = \frac{1}{\sin\phi}\left[\ln\left(\sin\frac{\theta+\phi}{2} - \ln\sin\frac{\theta-\phi}{2}\right)\right]_{\phi_h}^{\phi-\epsilon}$$

$$= \frac{1}{\sin\phi}\left[\ln\left|\sin\left(\frac{\phi-\epsilon}{2}\right)\right| - \ln\left|\sin\frac{\phi_h+\phi}{2}\right| - \ln\left|\sin\frac{(-\epsilon)}{2}\right| + \ln\left|\sin\frac{(\phi_h-\phi)}{2}\right|\right]$$

and $$\int_{\phi+\epsilon}^{\pi} \frac{d\theta}{\cos\theta - \cos\phi} = \frac{1}{\sin\phi}\left[\ln\left|\sin\frac{\epsilon}{2}\right| - \ln\left|\sin\phi + \frac{\epsilon}{2}\right|\right]$$

Adding these integrals, we get

$$\frac{1}{\sin\phi}\left[\ln\left|\frac{\sin(\phi - \epsilon/2)}{\sin(\phi + \epsilon/2)}\right| + \ln\left|\frac{\sin\left(\frac{\phi_h-\phi}{2}\right)}{\sin\left(\frac{\phi_h+\phi}{2}\right)}\right|\right]$$

As $\epsilon \to 0$, this tends to

$$\frac{1}{\sin\phi}\ln\left|\frac{\sin\left(\frac{\phi_h-\phi}{2}\right)}{\sin\left(\frac{\phi_h+\phi}{2}\right)}\right|$$

$$\therefore \int_{\phi_h}^{\pi} \frac{d\theta}{\cos\theta - \cos\phi} = \frac{1}{\sin\phi}\ln\left|\frac{\sin\left(\frac{\phi_h-\phi}{2}\right)}{\sin\left(\frac{\phi_h+\phi}{2}\right)}\right|$$

(2) $$\int_0^{\pi} \cot\frac{\phi}{2}\sin\phi\, d\phi = \int_0^{\pi}(1+\cos\phi).\, d\phi = \pi$$

(3) $$\int_{\phi_h}^{\pi} \cot\frac{\phi}{2}(\cos\phi_h - \cos\phi).\sin\phi\,.\,d\phi$$

$$= \int_{\phi_h}^{\pi}(\cos\phi_h - \cos\phi)d\phi + \int_{\phi_h}^{\pi}(\cos\phi_h - \cos\phi)\cos\phi\, d\phi$$

$$= \cos\phi_h(\pi - \phi_h) + \sin\phi_h + \int_{\phi_h}^{\pi}(\cos\phi_h - \cos\phi)\, d(\sin\phi)$$

$$= (\pi - \phi_h)(\cos\phi_h - \tfrac{1}{2}) + \sin\phi_h - \frac{\sin 2\phi_h}{4}$$

(4) Differential of $\ln \left| \dfrac{\sin\left(\frac{\phi_h + \phi}{2}\right)}{\sin\left(\frac{\phi_h - \phi}{2}\right)} \right|$

$$= \frac{\sin\left(\frac{\phi_h - \phi}{2}\right)}{\sin\left(\frac{\phi_h + \phi}{2}\right)} \left| \frac{\sin\frac{\phi_h - \phi}{2} \cos\frac{\phi_h + \phi}{2} + \sin\frac{\phi_h + \phi}{2} \cos\frac{\phi_h - \phi}{2}}{\sin^2 \frac{\phi_h - \phi}{2}} \right| d\phi$$

which, on reduction, equals

$$\frac{\sin \phi_h}{\cos \phi - \cos \phi_h} \, d\phi$$

(5) Evaluation of Integral

$$\int_0^{\phi_1} \ln \left| \frac{\sin\frac{\phi_h + \phi}{2}}{\sin\frac{\phi_h - \phi}{2}} \right| \sin\phi \, d\phi$$

$$= - \int_0^{\phi_1} \ln \left| \frac{\sin\frac{\phi_h + \phi}{2}}{\sin\frac{\phi_h - \phi}{2}} \right| d(\cos\phi)$$

$$= - \ln \left| \frac{\sin\frac{\phi_h + \phi}{2}}{\sin\frac{\phi_h - \phi}{2}} \right| \cos\phi \Bigg|_0^{\phi_1} + \int_0^{\phi_1} \frac{\cos\phi \sin\phi_h}{\cos\phi - \cos\phi_h} \, d\phi$$

This second integral is Glauert's integral if $\phi_1 = \pi$.

For general case

$$= \int_0^{\phi_1} \left(1 + \frac{\cos\phi_h}{\cos\phi - \cos\phi_h}\right) d\phi = \phi_1 + \cos\phi_h \int_0^{\phi_1} \frac{d\phi}{\cos\phi - \cos\phi_h}$$

As in Section 1 this integral can be evaluated as

$$\frac{1}{\sin\phi} \cdot \ln \left| \frac{\sin \frac{\phi_h + \phi_1}{2}}{\sin \frac{\phi_h - \phi_1}{2}} \right|$$

$$\therefore \int_0^{\phi_1} \ln \left| \frac{\sin \frac{\phi_h + \phi}{2}}{\sin \frac{\phi_h - \phi}{2}} \right| \sin\phi \; d\phi = \phi_1 \sin \phi_h + (\cos \phi_h - \cos\phi_1) \ln \left| \frac{\sin \frac{\phi_h + \phi}{2}}{\sin \frac{\phi_h - \phi}{2}} \right|$$

When $\phi_1 = \pi$, this reduces to $\pi \sin \phi_h$

$$(6) \quad \int_{\phi_h}^{\pi} \ln \left| \frac{\sin \frac{\phi_h + \phi}{2}}{\sin \frac{\phi_h - \phi}{2}} \right| (\cos\phi_h - \cos\phi) \sin\phi \; d\phi$$

$$= \int_{\phi_h}^{\pi} (\cos \phi_h - \cos\phi) \; d \left[\phi \sin \phi_h + (\cos \phi_h - \cos\phi) \ln \left| \frac{\sin \frac{\phi_h + \phi}{2}}{\sin \frac{\phi_h - \phi}{2}} \right| \right]$$

Integrating this by parts

$$(\cos \phi_h - \cos\phi) \, \phi \sin \phi_h + (\cos \phi_h - \cos \phi)^2 \ln \left| \frac{\sin \frac{\phi_h + \phi}{2}}{\sin \frac{\phi_h - \phi}{2}} \right| \Bigg|_{\phi_h}^{\pi}$$

$$- \int_{\phi_h}^{\pi} \left[\phi \sin \phi_h + (\cos \phi_h - \cos \phi) \ln \left| \frac{\sin \frac{\phi_h + \phi}{2}}{\sin \frac{\phi_h - \phi}{2}} \right| \right] \sin\phi \; d\phi$$

$$= (\cos\phi_h - \cos\phi)\sin\phi_h\,\phi + (\cos\phi_h - \cos\phi)^2 \ln\left|\frac{\sin\frac{\phi_h+\phi}{2}}{\sin\frac{\phi_h-\phi}{2}}\right|\Bigg|_{\phi_h}^{\pi}$$

$$-\int_{\phi_h}^{\pi} \phi\sin\phi_h \sin\phi\, d\phi - \int_{\phi_h}^{\pi} (\cos\phi_h - \cos\phi)\ln\left|\frac{\sin\frac{\phi_h+\phi}{2}}{\sin\frac{\phi_h-\phi}{2}}\right| \sin\phi\, d\phi$$

$$\therefore 2\int_{\phi_h}^{\pi} (\cos\phi_h - \cos\phi)\ln\left|\frac{\sin\frac{\phi_h+\phi}{2}}{\sin\frac{\phi_h-\phi}{2}}\right| \sin\phi\, d\phi$$

$$= (\cos\phi_h - \cos\phi)^2 \ln\left|\frac{\sin\frac{\phi_h+\phi}{2}}{\sin\frac{\phi_h-\phi}{2}}\right|\Bigg|_{\phi_h}^{\pi} - \sin\phi\sin\phi_h + \phi\sin\phi_h\cos\phi_h$$

When evaluated over the range $\phi_h - \pi$ a question of convergence of the logarithmic term arises at ϕ_h. The logarithmic term vanishes at $\phi = \pi$, and also $\phi = \phi_h$.

$$\therefore \int_{\phi_h}^{\pi} (\cos\phi_h - \cos\phi)\ln\left|\frac{\sin\frac{\phi_h+\phi}{2}}{\sin\frac{\phi_h-\phi}{2}}\right| \sin\phi\, d\phi$$

$$= \frac{\pi - \phi_h}{2}\sin\phi_h\cos\phi_h + \frac{\sin^2\phi_h}{2}$$

APPENDIX II

The Evaluation of k

From equation (42)

$$k = \frac{2}{\pi(1-E)} \int_0^{\pi} \left(\cot\frac{\phi}{2} - \frac{1}{\sin\phi_h} \ln \left| \frac{\sin\frac{\phi_h+\phi}{2}}{\sin\frac{\phi_h-\phi}{2}} \right| \right) \left\{ 1 + \frac{2X-1+\cos\phi}{\sqrt{(2X-1+\cos\phi)^2+4Y^2}} \right\} \sin\phi \, d\phi$$

$$= \frac{2}{\pi(1-E)} \int_0^{\pi} \cot\frac{\phi}{2} \sin\phi \left\{ 1 + \frac{2X-1+\cos\phi}{\sqrt{(2X-1+\cos\phi)^2+4Y^2}} \right\} \sin\phi \, d\phi$$

$$- \frac{2}{\pi(1-E)\sin\phi_h} \int_0^{\pi} \ln \left| \frac{\sin\frac{\phi_h+\phi}{2}}{\sin\frac{\phi_h-\phi}{2}} \right| \left\{ 1 + \frac{2X-1+\cos\phi}{\sqrt{(2X-1+\cos\phi)^2+4Y^2}} \right\} \sin\phi \, d\phi$$

$$= \frac{2}{(1-E)} i(XY) - \frac{2}{\pi(1-E)\sin\phi_h} (\pi \sin\phi_h) \quad \text{See Appendix I}$$

$$- \frac{2}{\pi(1-E)\sin\phi_h} \int_0^{\pi} \ln \left| \frac{\sin\frac{\phi_h+\phi}{2}}{\sin\frac{\phi_h-\phi}{2}} \right| \sin\phi \left\{ \frac{2X-1+\cos\phi}{\sqrt{(2X-1+\cos\phi)^2+4Y^2}} \right\} d\phi$$

$$= \frac{2}{(1-E)} i(XY) - \frac{2}{1-E} - \frac{2k}{\pi(1-E)\sin\phi_h}$$

where

$$k = \int_0^{\pi} \ln \left| \frac{\sin\frac{\phi_h+\phi}{2}}{\sin\frac{\phi_h-\phi}{2}} \right| \sin\phi \left\{ \frac{2X-1+\cos\phi}{\sqrt{(2X-1+\cos\phi)^2+4Y^2}} \right\} d\phi$$

k is determined graphically.

APPENDIX III

Two-dimensional Properties of Flapped Plates

It is interesting to note that the logarithmic distribution has a C_L contribution.

$$C_L c = \frac{\pi a_1}{4} = 2\delta \sin \phi_h$$

$$\therefore C_M = -\frac{(1 - E)}{2} \cdot C_L c$$

This implies that the centre of pressure is $\frac{1 - E}{2}$ behind the quarter chord point, or

$$X_{cp} = .25 + \frac{1 - E}{2}$$ for camber line distribution. (Fig. 3).

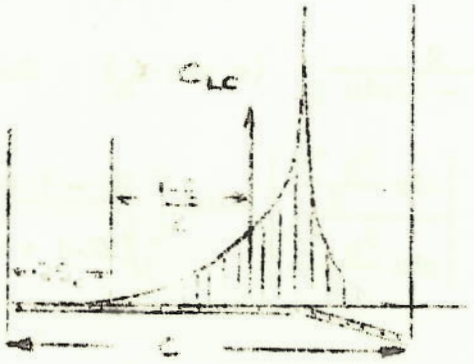

Fig. 17.

From this we see that the logarithmic distribution has its centre of area, or centre of pressure forward of the hinge line. Also, the centre of pressure for the whole flapped plate distribution may be estimated for zero geometric incidence.

$$X_{c.p.} = \frac{1}{4} + \frac{C_M}{C_L} = \frac{1}{4} + \frac{a_1 (1 - E)}{4(a_o + a_{1/2})}$$

$$= \frac{1}{4}\left(1 + \frac{2 \sin \phi_h (1 - E)}{\pi - \phi_h + \sin \phi_h}\right)$$

Note: The centre of pressure of flapped aerofoil does not change with δ, but is a function of ϕ_h . It is always behind the quarter chord point, and ahead of mid-chord for trailing edge flaps.

The hinge moment, H, can be calculated, using the logarithmic function.

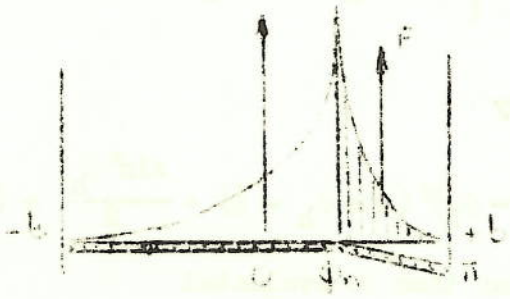

Fig. 18.

$$H = \int_{x_h}^{b} P(x)\,(x - x_h)\,dx \qquad C_H = \frac{H}{\rho'_2\, V^2 (2b)^2\, E},$$

where P(x) is the pressure normal to the chord at the point x.

$$\therefore \quad C_H = \frac{1}{\rho'_2 V^2\, 4E} \int_{x_h}^{1} P(x)\,(\bar{x} - \bar{x}_h)\,d\bar{x} = \frac{1}{4E} \int_{\phi_h}^{\pi} \ell(\phi)(\cos\phi_h - \cos\phi) \sin\phi \; d\phi$$

This integral is evaluated in Appendix I to give

$$C_H = \frac{\delta}{E\pi}\left(\frac{\pi - \phi_h}{2} \sin\phi_h \cos\phi_h + \frac{\sin^2\phi_h}{2}\right)$$

$$= \frac{1}{E}\left(a_o\, a_2 + \frac{a_1^2}{128}\right)$$

Including the hinge moment due to the induced $\cot\frac{\phi}{2}$ distribution

$$C_{Hi} = \frac{\delta}{E}\left(\frac{\pi-\phi_h}{\pi}\right)\int_{\phi_h}^{\pi} \cot\frac{\phi}{2}\,(\cos\phi_h - \cos\phi)\,\sin\phi\; d\phi$$

which from Appendix I becomes

$$= \frac{\delta}{E}\left(\frac{\pi-\phi_h}{\pi}\right)\left[(\pi-\phi_h)(\cos\phi_h - \tfrac{1}{2}) + \sin\phi_h - \frac{\sin 2\phi_h}{4}\right]$$

The total C_H is given by

$$C_H = \frac{\delta}{\pi E}\left[(\pi-\phi_h)^2(\cos\phi_h - \tfrac{1}{2}) + \frac{\sin^2\phi_h}{2} + (\pi-\phi_h)\sin\phi_h\right]$$

The usual derivatives may then be evaluated

$$b_2 = \frac{\partial C_H}{\partial\delta} = \frac{1}{\pi E}\left[(\pi-\phi_h)^2(\cos\phi_h - \tfrac{1}{2}) + \frac{\sin^2\phi_h}{2} + (\pi-\phi_h)\sin\phi_h\right]$$

$$m = \frac{\partial C_M}{\partial\delta} = -\frac{\sin\phi_h}{2}(1-\cos\phi_h)$$

$$a_2 = \frac{\partial C_L}{\partial\delta} = 2\left(\pi-\phi_h + \frac{4\sin\phi_h}{\pi}\right)$$

Experimental values of these derivatives[6] are roughly 20% lower than those calculated from the above formulae.

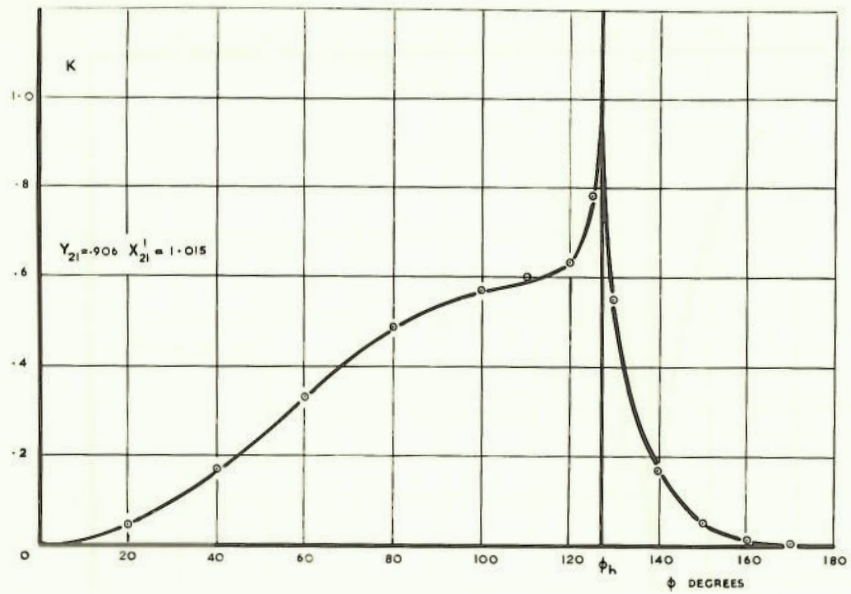

FIG. 5. METHOD OF GRAPHICAL INTEGRATION.

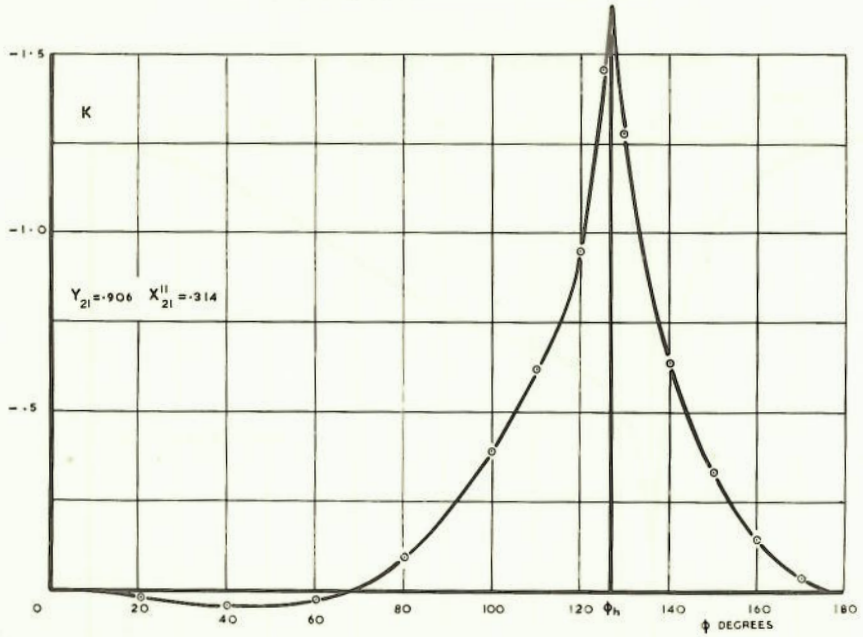

FIG. 6. METHOD OF GRAPHICAL INTEGRATION

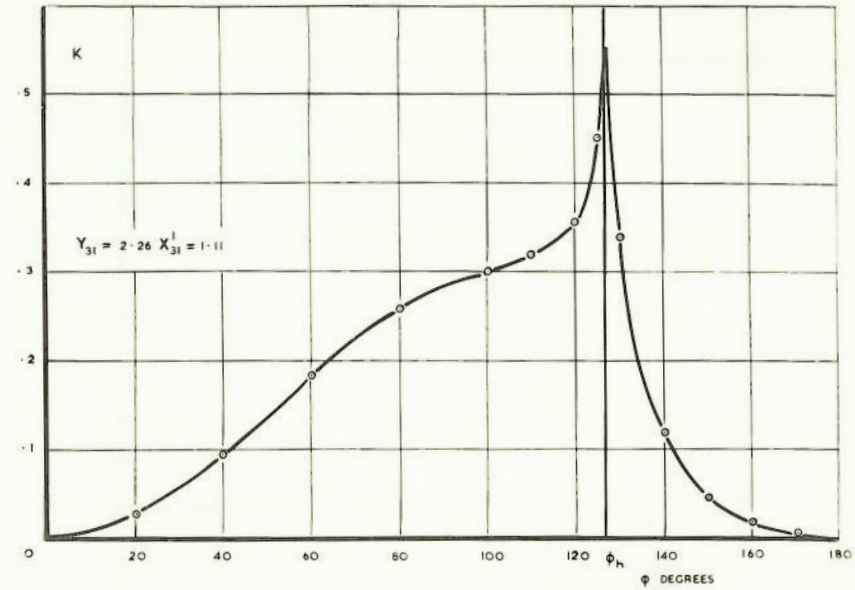

FIG. 7. METHOD OF GRAPHICAL INTEGRATION.

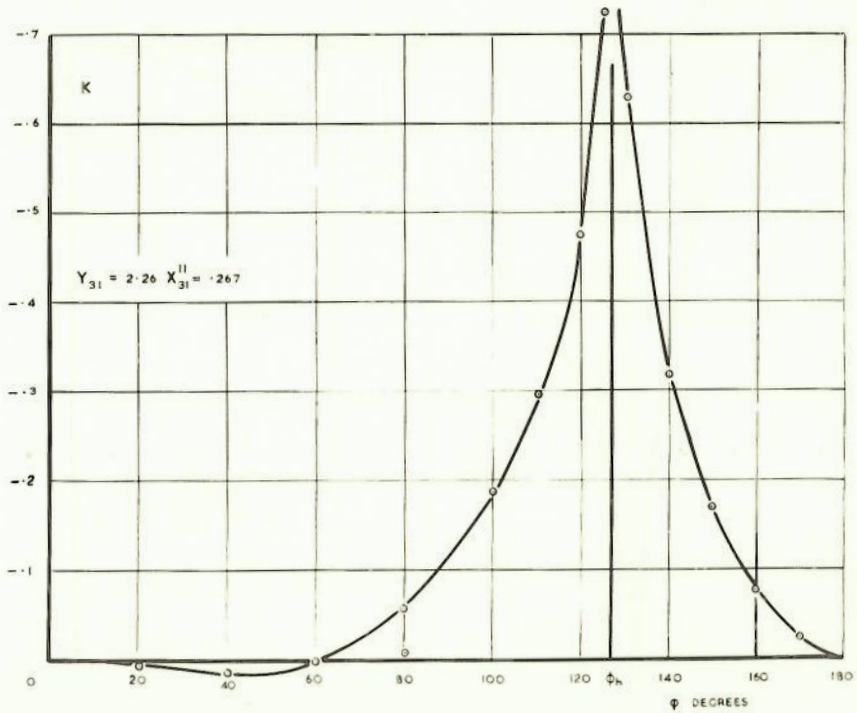

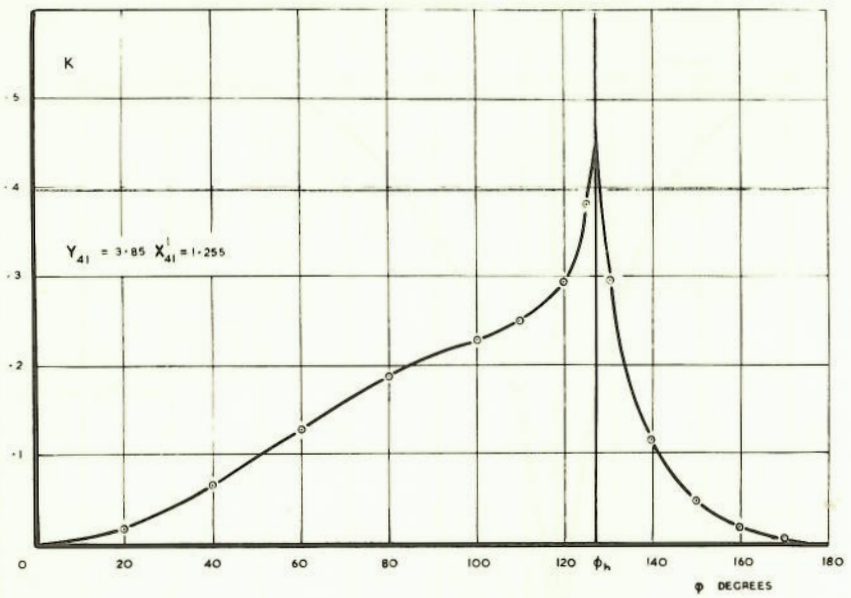

FIG. 9. METHOD OF GRAPHICAL INTEGRATION

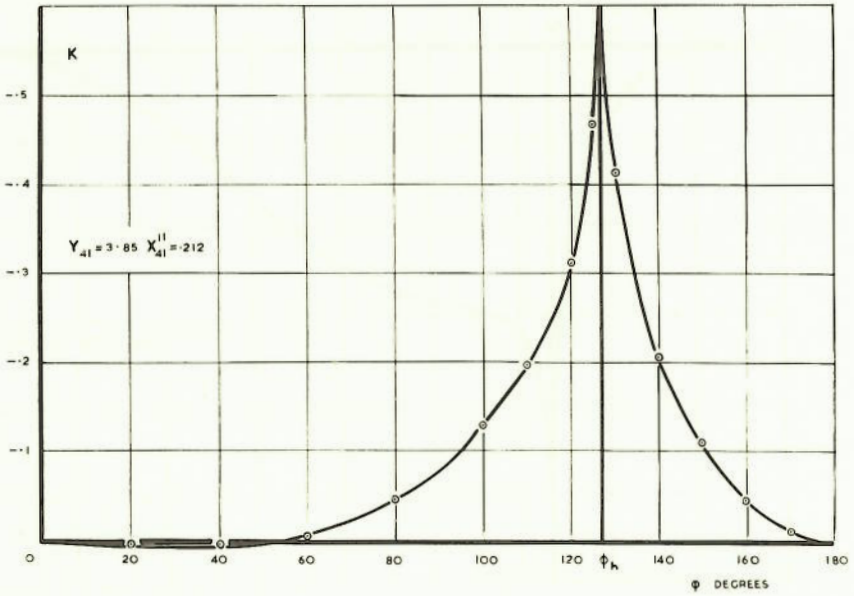

FIG. 10. METHOD OF GRAPHICAL INTEGRATION.

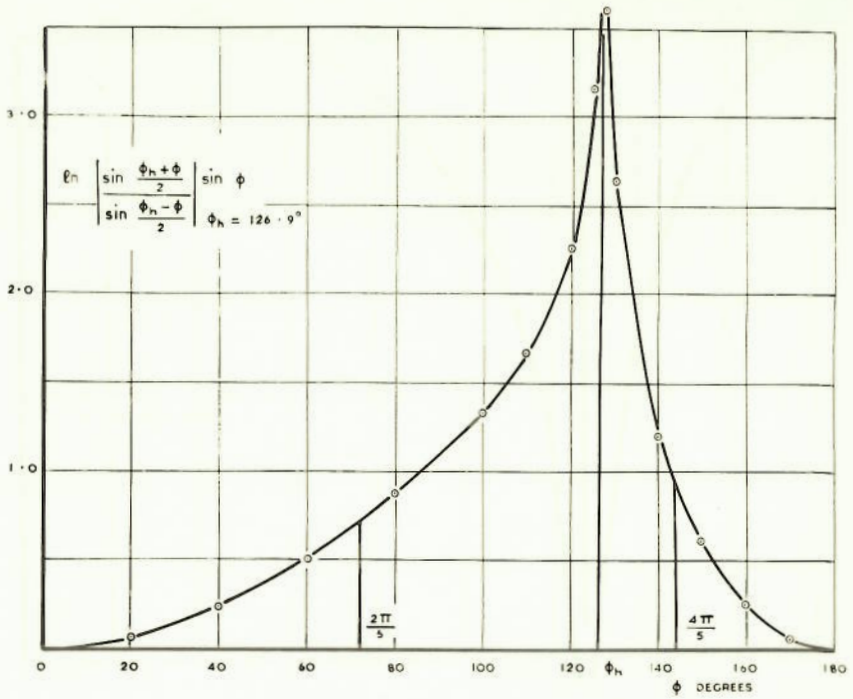

FIG. 11. METHOD OF GRAPHICAL INTEGRATION.

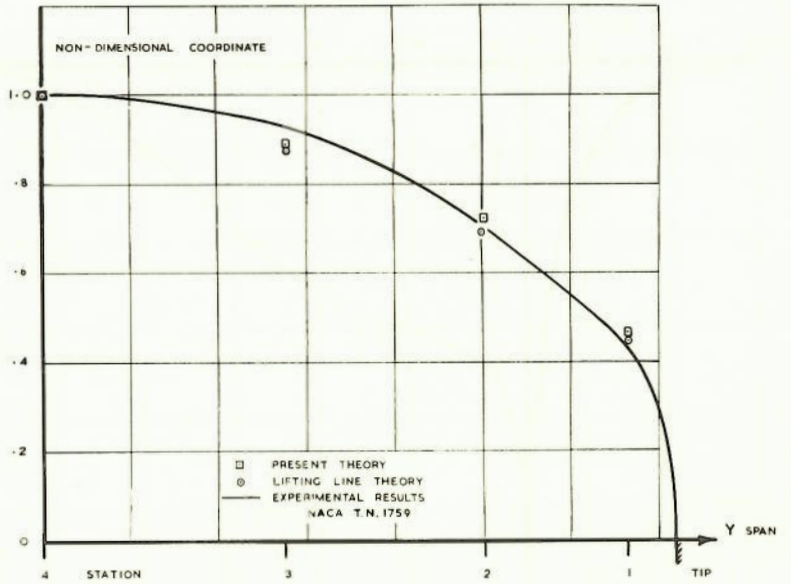

FIG. 12. SPANWISE SHAPE OF LIFT DISTRIBUTION

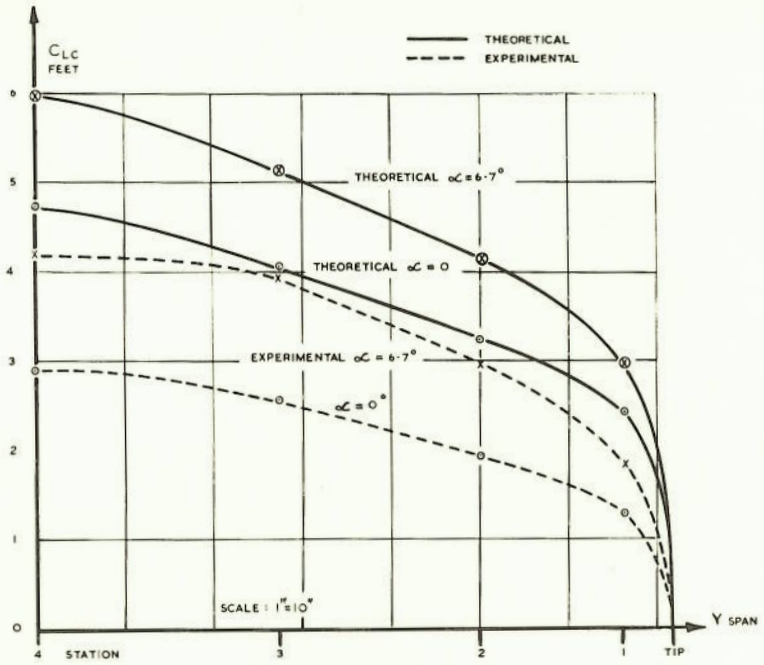

FIG. 13. SPANWISE VARIATION OF LIFT.

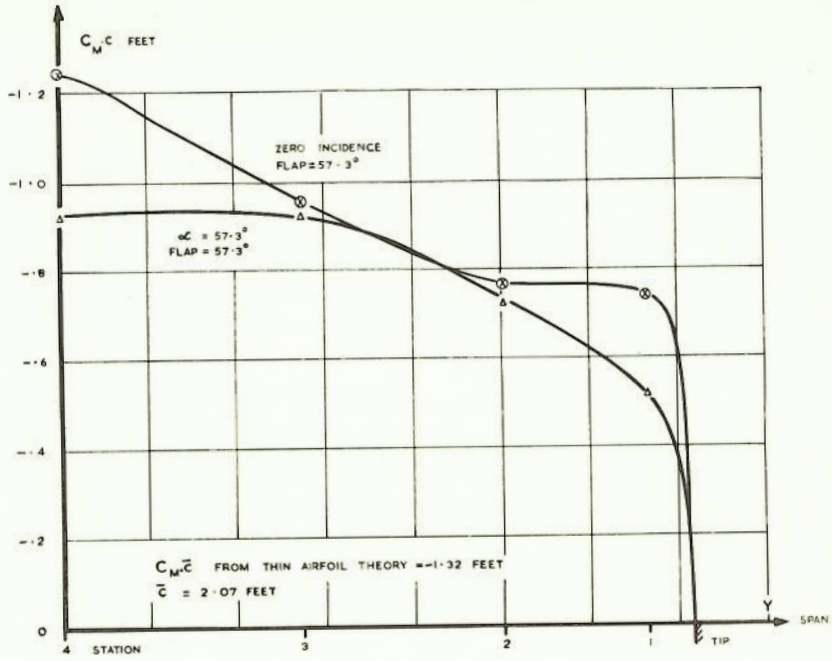

FIG. 15. SPANWISE MOMENT VARIATION.

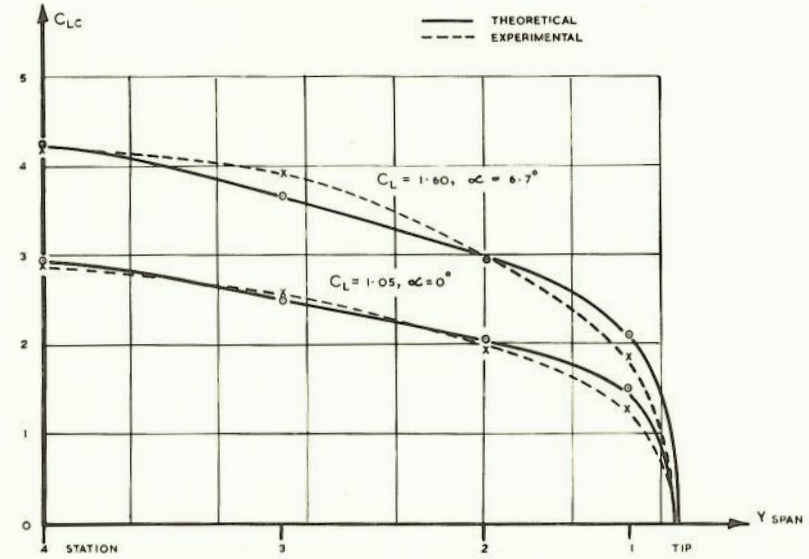

FIG. 14. SPANWISE LIFT DISTRIBUTION FOR EQUAL WING C_L.

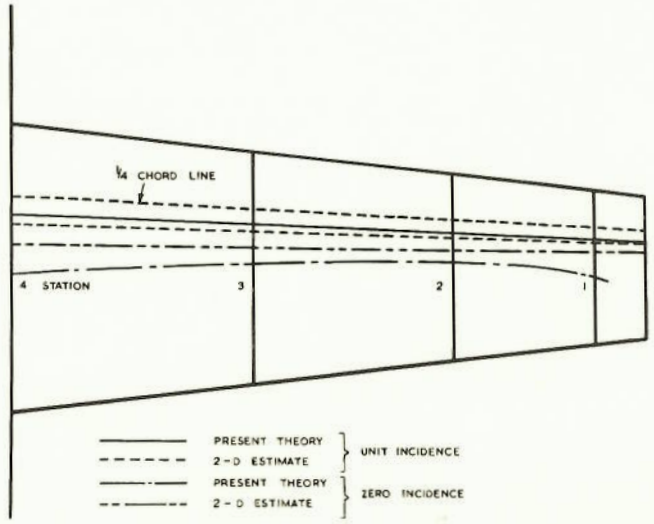

FIG. 16. VARIATION IN CENTRE OF PRESSURE.

TABLE 1

$$\ln \left| \frac{A \sin \frac{\phi}{2} + B \cos \frac{\phi}{2}}{A \sin \frac{\phi}{2} - B \cos \frac{\phi}{2}} \right| \sin \phi$$

$\phi_h = 180 - 53.1 = 126.9$

$A = \cos 63.5 = .446$

$B = \sin 63.5 = .895$

ϕ	$\phi/2$	$\sin \phi/2$	$\cos \phi/2$	$A \sin \phi/2$	$B \cos \phi/2$	Sum	Diff	Quot.	$\ln_e \lvert Quot \rvert$	$\sin \phi$	$\ln \lvert - \lvert \sin \phi$
20	10	.1736	.9848	.078	.881	.959	.803	1.19	.1739	.3420	.0594
40	20	.3420	.9397	.152	.840	.992	.688	1.44	.3646	.6428	.2340
60	30	.500	.8660	.223	.775	.998	.552	1.80	.5877	.8660	.509
80	40	.6428	.7660	.287	.685	.972	.398	2.44	.8919	.9848	.876
100	50	.7660	.6428	.342	.575	.917	.237	3.86	1.3506	.9848	1.33
110	55	.8190	.5730	.365	.513	.878	.148	5.94	1.7817	.9400	1.670
120	60	.8660	.500	.386	.447	.833	.061	13.65	2.614	.8660	2.260
125	62.5	.8870	.462	.396	.413	.809	.017	47.50	3.860	.8190	3.160
130	65	.905	.422	.403	.378	.781	.025	31.20	3.44	.7660	2.640
140	70	.9397	.342	.418	.306	.724	.112	6.45	1.8640	.6428	1.20
128	64	.900	.439	.401	.393	.794	.008	99.5	4.600	.788	3.62
150	75	.966	.259	.431	.232	.663	.199	3.33	1.2029	.500	.601
160	80	.9848	.1736	.439	.156	.595	.283	2.10	.7419	.3420	.253
170	85	.9962	.0872	.445	.078	.523	.367	1.43	.3577	.1736	.062

TABLE 2

$\nu = 2$, $n = 1$

$Y = .906$ $X' = 1.015$

				(1)	(2)	(3)	(4)	(5)	(6)			
ϕ	$\sin\phi$	$\cos\phi$	$\ln \lvert\lvert \sin\phi$	$2X+\cos\phi$	$(1)-1$	$(2)^2$	$(3)+4Y^2$	$(4)^{V_2}$	$(2)/(5)$	$(6)\ln \lvert\lvert$	$\sin\phi$	$(6)\ln \lvert\lvert \sin$
			2.03				3.28					
20	.342	.940	.0403	2.970	1.97	3.89	7.17	2.68	.735	.0594	.0296	.0436
40	.643	.766	.156	2.796	1.796	3.22	6.50	2.55	.702	.234	.109	.165
60	.866	.500	.337	2.530	1.53	2.34	5.62	2.37	.645	.509	.217	.328
80	.985	.174	.564	2.204	1.204	1.45	4.73	2.17	.555	.876	.313	.486
100	.985	-.174	.828	1.856	0.856	.73	4.01	2.00	.428	1.27	.354	.569
110		-.342		1.69	.69	.476	3.76	1.94	.356	1.67		.595
120	.866	-.500	1.14	1.530	.530	.28	3.56	1.89	.280	2.26	.319	.633
130	.766	-.643	1.38	1.387	.387	.15	3.43	1.85	.209	2.64	.289	.552
140	.643	-.766	2.02	1.264	.264	.07	3.35	1.83	.144	1.20	.291	.173
142	.616	-.788	2.53	1.242	.242	.058	3.34	1.83	.132		.334	
145	.574	-.819	2.03	1.211	.211	.045	3.33	1.82	.116		.236	
150	.500	-.866	1.18	1.164	.164	.027	3.31	1.82	.090	.601	.106	.054
125		-.573		1.46	.46	.212	3.49	1.87	.246	3.16		.778
160	.342	-.940	.41	1.090	.090	.008	3.29	1.81	.050	.253	.020	.0125
170	.174	-.985	.094	1.045	.045	.002	3.28	1.81	.025	.062	.002(5)	.0015

TABLE 3

CALCULATION OF X AND Y

$b/2 = \frac{144"}{2} = 72"$

STA.	η_ν	C_ν	Y_ν	$X_{L.E.}$	x''_ν	x'_ν	b/x_ν	$\lvert\eta_\nu - \eta_1\rvert$	$\lvert\eta_\nu - \eta_2\rvert$	$\lvert\eta_\nu - \eta_3\rvert$	$\lvert\eta_\nu - \eta_4\rvert$
1	.9239	17.2	$\frac{133}{2}$	- 8.6	-2.66	+ 6.95	4.18	0	.2168	.5412	.9239
2	.7071	20.7	$\frac{101.5}{2}$	-10.35	-3.2	+ 8.85	3.48	.2168	0	.3144	.7071
3	.3827	25.9	$\frac{55.1}{2}$	-12.95	-4.02	+10.45	2.78	.5412	.3144	0	.3827
4	0	32	0	-16	-4.95	+12.95	2.25	.9239	.7071	.3827	0

$x''_\nu - x_{n.L.E.}$

n =	1	2	3	4
1	5.94	7.69	10.29	13.34
2	5.4	7.15	9.75	12.8
3	4.58	6.33	8.93	11.98
4	3.65	5.4	8.0	11.05

$x'_\nu - x_{n.L.E.}$

n =	1	2	3	4
1	15.55	17.30	19.9	22.95
2	17.45	19.20	20.8	24.85
3	19.05	20.8	23.4	26.45
4	21.55	23.3	25.9	28.95

TABLE 4

Y, X VALUES

		X''				X'				
STA. ν	n =	1	2	3	4	1	2	3	4	$X_{\nu n} = X_{-\nu n}$
1		.345	.371	.397	.417	.905	.835	.767	.716	
2		.314	.345	.376	.40	1.015	.925	.801	.775	
3		.267	.306	.345	.373	1.11	1.0	.905	.825	
4		.212	.261	.309	.345	1.255	1.125	1.0	.905	

Y

	n	1	2	3	4
1	0	0	.754	1.5	2.065
2		.906	0	.875	1.59
3		2.26	1.095	0	.861
4		3.85	2.46	1.065	0
-3			3.79		.861
-2		6.80		3.03	
-1			5.69		2.07

TABLE 5

TABULATION OF k

STA ν	n	k (X″) 1	2	3	4	k (X′) 1	2	3	4
1			-.802	-.415	-.230		.525	.185	.0655
2		-.842		-.694	-.390	.870		.381	.195
3		-.414	-.700		-.725	.490	.721		.455
4		-.281	-.387	-.706		.385	.470	.741	
-3			-.203		-.725		.227		.455
-2		-.120		-.169		.134		.123	
-1			-.120		-.230		.0815		.0655

TABLE 6

INFLUENCE FUNCTIONS $i(X'', Y)$ $i(X', Y)$, $I_{\nu\nu}$

STATION ν	n	i(X″ Y) 1	2	3	4	i(X′ Y) 1	2	3	4
1		1.575	1.15	1.20	1.15	2.081	1.58	1.30	1.25
2		1.075	1.913	1.14	1.12	1.61	2.289	1.50	1.35
3		1.0	1.06	1.978	1.13	1.35	1.54	2.330	1.52
4		1.0	1.0	1.06	1.844	1.25	1.35	1.56	2.247
-3			1.05		1.13		1.20		1.52
-2		1.00		1.10		1.12		1.20	
-1			1.05		1.15		1.10		1.25

TABLE 7

LOGARITHMIC CORRECTION $\Delta i_{\nu\nu} = 4k_1 (\frac{b}{2c_\nu})^2 F(\theta)$, etc.

$k'_1 = 1.20$ $k'_3 = -22.7$
$k''_1 = 1.94$ $k''_3 = +8.50$

ν	$b/2c_\nu$	$(b/2c_\nu)^2$	$F(\theta)$	$4k''_1$	$\Delta i''_{\nu\nu}$	$\bar{i}''_{\nu\nu}$	$4k'_1$	$\Delta i'_{\nu\nu}$	$\bar{i}'_{\nu\nu}$
1	4.18	17.5	.00125	7.76	.170	1.575	4.80	.106	2.081
2	3.48	12.1	.00542	7.76	.508	1.913	4.80	.314	2.289
3	2.78	7.71	.00958	7.76	.573	1.978	4.80	.355	2.330
4	2.25	5.01	.01130	7.76	.439	1.844	4.80	.272	2.247
				$4k''_3$	$\Delta k''_{\nu\nu}$	$\bar{k}''_{\nu\nu}$	$4k'_3$	$\Delta k'_{\nu\nu}$	$\bar{k}'_{\nu\nu}$
1				34	.743	3.62	-90.8	-1.98	-1.70
2				34	2.23	5.11	-90.8	-5.95	-5.66
3				34	2.51	5.39	-90.8	-6.70	-6.41
4				34	1.92	4.80	-90.8	-5.14	-4.85

$k''(X0) = 2.88$ $k'(X0) = .236$

TABLE 8

INFLUENCE FUNCTIONS $k(X''Y)\, k(X'Y)\, \bar{k}_{\nu\nu}$

STA ν	n	$k(X''Y)$ 1	2	3	4	$k(X'Y)$ 1	2	3	4
1		3.62	1.17	.912	.480	-1.70	.925	.565	.560
2		1.02	5.11	1.04	.687	.660	-5.66	.870	.680
3		.413	.845	5.39	1.05	.388	.633	-6.41	.598
4		.280	.385	.850	4.80	.242	.408	0.662	-4.85
-3			.328		1.05		.262		.598
-2		.121		.418		.180		.375	
-1			.247		.480		.180		.560

TABLE 9

$\phi_{\nu n}$ VALUES

ν	n	1	2	3	4
1		.1913	.3599	0	.028
2		.3599	.3536	.3879	0
3		0	.3879	.4619	.3943
4		.028	0	.3943	0.5
-3		0	.0344	0	.3943
-2		.0064	0	.0344	0
-1		0	.0064	0	.028

TABLE 10

FORM I

ν or n	±1	±2	±3	
$I'_{\nu\nu}$	2.081	2.289	2.330	2.247
$I''_{\nu\nu}$	1.575	1.913	1.978	1.844
$K'_{\nu\nu}$	-1.70	-5.66	-6.41	-4.85
$K''_{\nu\nu}$	3.62	5.11	5.39	4.80
$I'_{\nu\nu} K''_{\nu\nu}$	7.53	11.70	12.55	10.80
$I''_{\nu\nu} K'_{\nu\nu}$	-2.68	-10.85	-12.70	-8.94
$I'_{\nu\nu} K''_{\nu\nu} - I''_{\nu\nu} K'_{\nu\nu}$	10.21	22.55	25.25	19.74
ℓ'_ν	.354	.227	.213	.243
ℓ''_ν	-.165	-.251	-.254	-.246
m'_ν	.154	.085	.078	.093
m''_ν	.204	.102	.092	.114

where

$$\ell'_\nu = \frac{K''_{\nu\nu}}{I''_{\nu\nu} K'_{\nu\nu} - I'_{\nu\nu} K''_{\nu\nu}}$$

$$\ell''_\nu = \frac{K'_{\nu\nu}}{I''_{\nu\nu} K'_{\nu\nu} - I'_{\nu\nu} K''_{\nu\nu}}$$

$$m''_\nu = \frac{I'_{\nu\nu}}{I''_{\nu\nu} K'_{\nu\nu} - I'_{\nu\nu} K''_{\nu\nu}}$$

$$m'_\nu = \frac{I''_{\nu\nu}}{I''_{\nu\nu} K'_{\nu\nu} - I'_{\nu\nu} K''_{\nu\nu}}$$

TABLE 11 PART II

	n ODD (1)		(3)		EVEN (2)		(4)	
ν	2	4	2	4	1	3	1	3
$a_{\nu n}\ i'_{\nu n}$	.578	.035	.583	.615	.568	.597	.035	.600
$a_{\nu n}\ i''_{\nu n}$	.382	.028	.442	.418	.414	.411	.032	.445
$a_{\nu n}\ k''_{\nu n}$	.367	.0078	.404	.335	.420	.328	.0135	.415
$a_{\nu n}\ k'_{\nu n}$	.237	.0068	.338	.261	.333	.246	.0155	.236
$a_{\nu n}\ \ell'_\nu\ i'_{\nu n}$	.132	.0085	.132	.149	.201	.127	.0124	.128
$a_{\nu n}\ \ell''_\nu\ i''_{\nu n}$	-.096	-.0069	-.111	-.103	-.0683	-.104	-.00528	-.113
$a_{\nu n}(\ell'_\nu\ i'_{\nu n} - \ell''_\nu i''_{\nu n})$	.228	.0154	.243	.252	.269	.231	.0177	.241
$a_{\nu n}\ \ell'_\nu\ k'_{\nu n}$	.0538	.00165	.0768	.0635	.118	.0525	.0055	.0502
$a_{\nu n}\ \ell''_\nu\ k''_{\nu n}$	-.092	-.0019	-.101	-.0824	-.0692	-.0834	-.00222	-.105
$a_{\nu n}(\ell'_\nu\ k'_{\nu n} - \ell''_\nu k''_{\nu n})$	.1458	.0036	.178	.1459	.187	.1359	.0077	.1552
$a_{\nu n}\ m''_\nu\ i''_{\nu n}$	.0390	.00320	.0450	.0477	.0645	.0378	.00653	.0410
$a_{\nu n}\ m'_\nu\ i'_{\nu n}$	.0492	.00326	.0495	.0571	.0875	.0467	.0054	.0469
$a_{\nu n}(n''_\nu\ i'_{\nu n} - m'_\nu\ i'_{\nu n})$	-.0102	-.00006	-.0045	-.0106	-.0030	-.0089	.00113	-.0059
$a_{\nu n}\ m''_\nu\ k''_{\nu n}$	.0375	.00089	.0413	.0385	.0856	.0302	.00275	.0382
$a_{\nu n}\ m'_\nu\ k'_{\nu n}$	.0201	.00064	.0287	.0242	.0513	.0192	.00238	.0184
$a_{\nu n}\ (n''k''_{\nu n} - m'_\nu\ k'_{\nu n})$	.0174	.00025	.0126	.0143	.0343	.0112	.0004	.0198

TABLE 12 PART II

	n ODD (1)	(3)	n EVEN (2)		(4)	
ν	-2	-2	-3	-1	-3	-1
$a_{\nu n}\ i'_{\nu n}$	.00715	.0413	.0413	.00705	.600	.0349
$a_{\nu n}\ i''_{\nu n}$	.0064	.0378	.0361	.0067	.445	.0322
$a_{\nu n}\ k''_{\nu n}$	.000775	.0144	.0113	.00158	.414	.0134
$a_{\nu n}\ k'_{\nu n}$	.00115	.0129	.0090	.00115	.236	.0157
$a_{\nu n}\ \ell'_\nu\ i'_{\nu n}$	.00162	.0094	.0088	.0025	.128	.0124
$a_{\nu n}\ \ell''_\nu\ i''_{\nu n}$	-.0016	-.0095	-.00916	-.00110	-.113	-.00531
$a_{\nu n}(\ell'_\nu\ i'_{\nu n} - \ell''_\nu\ i''_{\nu n})$	.00322	.0189	.0180	.0036	.241	.0177
$a_{\nu n}\ \ell'_\nu\ k'_{\nu n}$	.00026	.00292	.00191	.000407	.0502	.00555
$a_{\nu n}\ \ell''_\nu\ k''_{\nu n}$	-.000195	-.00362	-.00267	-.000260	-.105	-.00259
$a_{\nu n}(\ell'_\nu\ k'_{\nu n} - \ell''_\nu\ k''_{\nu n})$	.00046	.00654	.00478	.000667	.1552	.00814
$a_{\nu n}\ m''_\nu\ i''_{\nu n}$	.000654	.00386	.00332	.00136	.0409	.00651
$a_{\nu n}\ m'_\nu\ i'_{\nu n}$	.000608	.00350	.00323	.00109	.0469	.00538
$a_{\nu n}(m''_\nu\ i''_{\nu n} - m'_\nu\ i'_{\nu n})$	.000046	.00036	.00009	.00025	-.0060	.00119
$a_{\nu n}\ m''_\nu\ k''_{\nu n}$	.00008	.00147	.00104	.000322	.038	.00274
$a_{\nu n}\ m'_\nu\ k'_{\nu n}$	.0000975	.00110	.00070	.000177	.0184	.00242
$a_{\nu n}(m''_\nu\ k''_{\nu n} - m'_\nu\ k'_{\nu n})$	-.000018	.00037	.00034	.000145	.0196	.00032

TABLE 13 $B_{\nu n}$ $D_{\nu n}$

	$B_{\nu n}$					$D_{\nu n}$			
ν / n	1	2	3	4	ν / n	1	2	3	4
2	.269		.231		2	-.0030		-.0089	
	.0036		.018			.00025		.00009	
	.273		.249			-.0027		-.0088	
4	.0177		.241		4	.00113		-.0060	
1		.228		.0154	1		-.0102		.00006
		.0032		.0154			.00004		.00006
		.2312		.0308			-.0102		-.00012
3		.243		.252	3		-.0045		-.0106
		.0189		.252			.00036		-.0106
		.2619		.504			-.0041		-.0212

TABLE 14

$C_{\nu n}$ $E_{\nu n}$

	$C_{\nu n}$				$E_{\nu n}$			
ν / n	1	2	3	4	1	2	3	4
2	.1870		.1359		.0343		.0112	
	.0048		.0048		.00015		.00034	
	.1822		.1407		.0343		.0115	
4	.0077		.1552		.00035		.0198	
1		.1458		.0036		.0174		.00025
		.0005				-.00001		
		.1463		.0072		.0174		.0005
3		.178		.1459		.0126		.0143
		.0065				.0004		
		.1845		.2918		.0130		.0206

TABLE 15 SUMMARY

$\alpha'' = 1$

$\alpha' = 2$

CALCULATION FOR UNIT INCIDENCE

ν	1	2	3	4	ν	1	2	3	4
y_ν	.2977	.4588	.5658	.6519	μ_ν	-.0214	-.0301	-.0386	-.0387
Δy_ν	-.00075	-.0025	-.0014	-.0040	$\Delta\mu_\nu$	+ 0	-.00004	+.00004	-.00001
	.2970	.4563	.5644	.6479		-.0214	-.0301	-.0386	-.0387
CHECKING									
$a_{\nu\nu}$	.1670	.2500	.3140	.3660		-.0199	-.0240	-.0296	-.0255
$B_{\nu n} y''$	.0115	.148	.156	.284		.000732	-.00231	-.0039	-.0120
$B_{\nu n} y'$	.125	.0685	.113	.00915		-.00123	-.00300	-.0040	-.0000356
$C_{\nu n} \mu''$	-.000298	-.0071	-.0060	-.0113		-.0000135	-.000501	-.000765	-.00110
$C_{\nu n} \mu'$	-.00547	-.00316	-.00423	-.000154		-.00103	-.000372	-.000348	-.0000108
	.2977	.4562	.5648	.6477		-.0214	-.0302	-.0386	-.0386

TABLE 16

$\alpha' = 2$

$\alpha'' = 1$

SOLUTION - EVEN ν

GUESS - $y_1 = .3$ $y_2 = .45$ $y_3 = .57$ $y_4 = .65$

$\mu_1 = -.02$ $\mu_2 = -.03$ $\mu_3 = -.035$ $\mu_4 = -.04$

ν	2	4	ν	2	4
$a_{\nu\nu}(2\ell'_\nu - \ell''_\nu)$	.2500	.3660	$a_{\nu\nu}(m''_{\nu\nu} - 2m'_\nu)$	-.0240	-.0255
$B_{\nu_3} y_3$	.149	.287	$D_{\nu_3} y_3$	-.00234	-.0121
$B_{\nu_1} y_1$	.0691	.00922	$D_{\nu_1} y_1$	-.00304	-.0000359
$C_{\nu_3} \mu_3$	-.00645	-.0102	$E_{\nu_3} \mu_3$	-.000455	-.0010
$C_{\nu_1} \mu_1$	-.00292	-.00014	$E_{\nu_1} \mu_1$	-.00034	-.00001
y_ν	.4588	.6519		-.0301	-.0387
$B_{\nu_3} \Delta y_3$	-.0011	-.00212	$D_{\nu_3} \Delta y_3$	+.000017	+.000088
$B_{\nu_1} \Delta y_1$	-.00053	-.000071	$D_{\nu_1} \Delta y_1$	+.000023	+ 0
$C_{\nu_3} \Delta\mu_3$	-.00066	-.00105	$E_{\nu_3} \Delta\mu_3$	-.0000465	-.000103
$C_{\nu_1} \Delta\mu_1$	-.000204	-.000010	$E_{\nu_1} \Delta\mu_1$	-.0000244	- 0
$\Delta y^{(1)}$	-.0025	-.0040	$\Delta\mu^{(1)}$	-.000037	-.000015

TABLE 17 ODD ν

$\alpha' = 2$

$\alpha'' = 1$

ν	1	3	ν	1	3
$a_{\nu\nu}(2\ell'_\nu - \ell''_\nu)$	.1670	.3140	$a_{\nu\nu}(2\ell'_\nu - \ell''_\nu)$	-.0199	-.0296
$B_{\nu_4}\ y_4$	.0115	.157	$D_{\nu_4}\ y_4$	.000735	-.00390
$B_{\nu_2}\ y_2$	.125	.115	$D_{\nu_2}\ y_2$	-.00124	-.00404
$C_{\nu_4}\ \mu_4$	-.000298	-.0060	$E_{\nu_4}\ \mu_4$	-.0000135	-.000765
$C_{\nu_2}\ \mu_2$	-.00548	-.00423	$E_{\nu_2}\ \mu_2$	-.00103	-.000346
y	.2977	.5658	μ	-.0214	-.0386
$\Delta y^{(1)}$	-.0023	-.0042	$\Delta \mu^{(1)}$	-.0014	-.0036
$B_{\nu_4}\ \Delta y_4$	-.000057	-.00077	$D_{\nu_4}\ y_4$	-.0000036	+.000019
$B_{\nu_2}\ ^{\circ}y_2$	-.00068	-.00062	$D_{\nu_2}\ y_2$	+.0000068	+.000022
$C_{\nu_4}\ \Delta\mu_4$	- 0	-.000002	$E_{\nu_4}\ \mu_4$	0	- 0
$C_{\nu_2}\ \Delta\mu_2$	-.000009	-.000007	$E_{\nu_2}\ \mu_2$	-.000002	- 0
	-.00075	-.00140		+.000003	+.000041

TABLE 18 SUMMARY

CALCULATION FOR ZERO INCIDENCE

$\alpha'' = 0$

$\alpha' = 1$

ν	1	2	3	4	ν	1	2	3	4
y_ν	.1026	.1361	.1692	.1974	μ_ν	-.0308	-.0327	-.0399	-.0517
$\Delta y^{(1)}$	-.0010	-.0006	-.0014	-.0007		+.00002	-.00005	+.00002	.00003
	.1016	.1355	.1678	.1967		-.0308	.0327	-.0399	-.0517
CHECKING									
$a_{\nu\nu}$	.0676	.080	.0965	.121		-.0295	-.030	-.036	-.047
$B_{\nu n}y''$	.00349	.044	.0475	.0845		.000222	-.000688	-.00118	-.00356
$B_{\nu n}y'$	.0370	.0235	.0338	.00312		-.000366	-.00103	-.00119	-.000012
$C_\nu\ \mu_1$	-.00040	-.00738	-.0080	-.0117		-.00001	-.000520	-.00102	-.00114
$C_\nu\ \mu_{11}$	-.00595	-.00450	-.0046	-.00022		-.00112	-.000535	-.000376	-.000015
	.1017	.1356	.1672	.1967		-.0308	-.0327	-.0398	-.0517

TABLE 19 SOLUTION ODD ν $\quad \alpha'' = 0$ $\quad \alpha' = 1$

GUESS $\quad \gamma_1 = .1 \quad \gamma_2 = .14 \quad \gamma_3 = .18 \quad \gamma_4 = .2$

$\mu_1 = -.028 \quad \mu_2 = -.033 \quad \mu_3 = -.04 \quad \mu_4 = -.05$

ν		1	3	ν	1	3
$a_{\nu\nu}\ \ell'_\nu\ \alpha'_\nu$		.0676	.0985	$-a_{\nu\nu}\ m'_\nu\ \alpha'_\nu$	-.0295	-.036
$B_{\nu_4}\ \gamma_4$		.0034	.0482		.000226	-.00120
$B_{\nu_2}\ \gamma_2$		.0380	.0349		-.000378	-.00123
$C_{\nu_4}\ \mu_4$		-.00039	-.0078		-.000017	-.00010
$C_{\nu_2}\ \mu_2$		-.0060	-.00464		-.00113	-.00038
	$\gamma^{(1)}$	.1026	.1692	μ	-.0308	-.03991
$B_{\nu_4}\ \Delta\gamma_4$		-.000046	-.000625		-.00000294	+.0000156
$B_{\nu_2}\ \Delta\gamma_2$		-.00106	-.00097		+.0000105	+.0000343
$C_{\nu_4}\ \Delta\mu_4$		-.00001	-.000264		-.00000059	-.0000338
$C_{\nu_2}\ \Delta\mu_2$		+.00006	.00045		+.000011	.000004
	$\Delta\gamma^{(2)}$	-.00105	-.0014	$\Delta\mu^{(2)}$	+.000018	+.0000201

TABLE 20 EVEN ν $\quad \alpha'' = 0$ $\quad \alpha' = 1$

ν		2	4	ν	2	4
$a_{\nu\nu}\ \ell'_\nu\ \alpha'_\nu$		.080	.121	$-a_{\nu\nu}m'_\nu\ \alpha'_\nu$	-.030	-.047
$B_{\nu_3}\ \gamma_3^{(1)}$		.0443	.0851		-.000693	-.00358
$B_{\nu_1}\ \gamma_1^{(1)}$		.0231	.00316		-.00104	-.0000123
$C_{\nu_3}\ \mu_3$		-.00736	-.0117		-.000520	-.00114
$C_{\nu_1}\ \mu_1$		-.00449	-.000222		-.000535	-.000015
		.1361	.1974		-.0327	-.0317
	$\Delta\gamma^{(1)}$	-.0039	-.0026	$\Delta\mu^{(1)}$	-.0003	+.0017
$B_{\nu_3}\ \Delta\gamma_3$		-.000366	-.00070		-.0000057	+.000030
$B_{\nu_1}\ \Delta\gamma_1$		-.00024	-.000032		+.000010	0
$C_{\nu_3}\ \Delta\mu_3$		.000004	.000006		0	.0000006
$C_{\nu_1}\ \Delta\mu_1$		.000003	0		0	0
		-.00060	-.00073		-.00005	.00003

TABLE 21

DETERMINATION OF CENTRE OF PRESSURE

STATION	UNIT INCIDENCE y	μ	$\frac{\mu/y}{C_M/C_L}$	$\frac{1}{4} - \frac{\mu}{y}$ x_{cp}	ZERO INCIDENCE y	μ	$\frac{\mu/y}{C_M/C_L}$	$\frac{1}{4} - \frac{x_{cp}}{}$
4	.6477	-.0386	-.0596	.3096	.1967	-.0517	-.263	.51
3	.5648	-.0386	-.0685	.3185	.1672	-.0398	-.238	.48
2	.4562	-.0302	-.0662	.3162	.1356	-.0327	-.241	.49
1	.2977	-.0214	-.0718	.3218	.1017	-.0308	-.303	.55

THEORETICAL 2D VALUE = .342

$\frac{C_M}{C_L} = .092$

THEORETICAL 2D VALUE = .422

$\frac{C_M}{C_L} = .172$

$\frac{C_M}{C_L}$ FROM EXP. $= \frac{-.24}{1.05} = -.229$

TABLE 22

COMPARISON OF C_L DISTRIBUTIONS

ZERO INCIDENCE α GEOMETRIC = 6.7° $C_N = 1.60$

STATION	EXPERIMENTAL $C_N.c'$	THEORY	DIFFERENCE	EXPERIMENTAL	THEORY	DIFFERENCE
1 TIP	1.28	2.44	1.16	1.83	2.98	1.15
2	1.93	3.25	1.32	2.95	4.16	1.21
3	2.57	4.03	1.46	3.94	5.14	1.20
4 ℄	2.90	4.73	1.83	4.20	5.97	1.77

TABLE 23

VARIATION OF C_M ACROSS THE SPAN

	ZERO INCIDENCE			$\alpha = 57.3^\circ$		
STATION	μ	C_{MC} FLAT	C_M	μ	C_{MC}	C_M
1	-.0308	-.740	-.515	-.0214	-.514	-.358
2	-.0327	-.785	-.455	-.0302	-.725	-.420
3	-.0398	-.955	-.442	-.0386	-.925	-.428
4	-.0517	-1.240	-.465	-.0386	-.925	-.346